POLITECNICO DI TORINO
Repository ISTITUZIONALE

About the design of float-ram, a manually operated press to produce compressed earth blocks for building construction

Original
About the design of float-ram, a manually operated press to produce compressed earth blocks for building construction / Tagliavini, L., Quaglia, G., Franco, W., Asteggiano, M.. - In: MECHANISM AND MACHINE THEORY. - ISSN 0094-114X. - ELETTRONICO. - 231:(2026), pp. 1-22. [10.1016/j.mechmachtheory.2026.106653]

Availability:
This version is available at: 11583/3016718 since: 2026-10-16T11:06:43Z

Publisher:
Elsevier

Published
DOI:10.1016/j.mechmachtheory.2026.106653

Terms of use:

This article is made available under terms and conditions as specified in the corresponding bibliographic description in the repository

Publisher copyright

(Article begins on next page)

25 October 2026

Mechanism and Machine Theory 231 (2026) 106653



Contents lists available at ScienceDirect

Mechanism and Machine Theory

journal homepage: www.elsevier.com/locate/mechmt



Research paper

About the design of float-ram, a manually operated press to produce compressed earth blocks for building construction

Luigi Tagliavini [a,*], Giuseppe Quaglia [a], Walter Franco [a], Matteo Asteggiano [b]

[a] Department of Mechanical and Aerospace Engineering, Politecnico di Torino, Corso Duca degli Abruzzi 29, Torino 10129, Piemonte, Italy
[b] Studio Tecnico Ing. Matteo Asteggiano, Strada della Colla 2, Pocapaglia 12060, Piemonte, Italy

ARTICLE INFO

Keywords:
Manually operate press
Mechanical design
Compressed earth blocks (CEBs)
Building construction
Open-source project

ABSTRACT

The right to adequate and sustainable housing remains an unresolved challenge worldwide. Self-construction techniques based on stabilized rammed earth represent an economically accessible, ecological, and efficient alternative to traditional wood-fired burnt bricks. This paper presents the mechanical design, experimental characterization, and socio-economic impact assessment of the Float-Ram manual press conceived for manufacturing the "Blocco Mattone", an interlocking stabilized compressed earth block. To overcome the constructive complexity, high cost, and ergonomic shortcomings of existing commercial bidirectional presses, Float-Ram features an innovative architecture based on a central cylindrical joint, a floating mold to achieve bidirectional compression and two cam-follower transmissions for the compression phase and the ejection of the block. The compression cam profile is designed to convert a constant input force into high compression forces with compression profiles that match experimental data on the compression of the soil mixture. Experimental laboratory testing conducted on a fully sensorized prototype validates the theoretical performance. Field deployment in Tanzania, including the construction of housing in Njombe, the Mkiu kindergarten, and the nursing school and hospital in Ikelu, demonstrates the technology's significant social impact.

1. Context of the research

Since its establishment in Article 25 of the *Universal Declaration of Human Rights* in 1948, the right to sufficient shelter has been acknowledged as a basic and fundamental human right. The right to sufficient housing has been addressed in various ways by other international treaties. In order to enhance everyone's quality of life, the United Nations *UN-Habitat* promotes socially and environmentally sustainable communities and cities [1]. In September 2015, the UN declared a new Agenda composed of seventeen Sustainable Development Goals [2]. Number eleven (SDG 11), titled *Make cities and human settlements inclusive, safe, resilient and sustainable*, has seven main targets. Among these targets, it is worth citing the number 11.1 *"ensure access for all to adequate, safe, and affordable housing and basic services and upgrade slums"*; and number 11.c *"Support least developed countries, including through financial and technical assistance, in building sustainable and resilient buildings utilizing local materials"*.

* Corresponding author.
E-mail addresses: luigi.tagliavini@polito.it (L. Tagliavini), giuseppe.quaglia@polito.it (G. Quaglia), walter.franco@polito.it (W. Franco), matteo@alisea.cn.it (M. Asteggiano).
URL: https://www.polito.it/en/staff?p=luigi.tagliavini (L. Tagliavini), https://www.polito.it/en/staff?p=giuseppe.quaglia (G. Quaglia), https://www.polito.it/en/staff?p=walter.franco (W. Franco)

https://doi.org/10.1016/j.mechmachtheory.2026.106653
Received 7 September 2026; Received in revised form 6 October 2026; Accepted 7 October 2026
Available online 14 October 2026
0094-114X/© 2026 The Author(s). Published by Elsevier Ltd. This is an open access article under the CC BY-NC-ND license (http://creativecommons.org/licenses/by-nc-nd/4.0/).

However, the complete application of the right to sufficient shelter is still a long way off. Over 1 billion people lived in slums in 2018, making up 24% of the urban population, a modest rise from 23% in 2014. There are 370 million slum dwellers in Eastern and South-Eastern Asia, 238 million in sub-Saharan Africa, and 226 million in Central and Southern Asia [2]. Regarding target 11.1, the SDGs 2025 report [3] shows that, worldwide, still 56.7% of urban population lives in slums, informal settlements or inadequate housing. Ten to fifteen million households in Latin America live in subpar housing, and the shortage of suitable housing keeps getting worse in this region. Only 1.5 million of the 2.5 million homes that are needed each year are constructed in a suitable manner [4].

Self-help housing practices in informal settlements, which house up to 60% of the urban population in some Latin American cities, are made possible by a persistent housing shortage [4]. In fact, it appears that low-cost construction technologies appropriate for self-construction [5], which make use of local, widespread, easily available, and inexpensive materials like straw [6–8], timber [9], or earth, may contribute to the mitigation of the problem due to the limited planning and financing capacities of public institutions, the ineffectiveness of assistance mechanisms, the lack of interest of private individuals, and the scarcity of resources on the part of single families.

Earth construction technology have been around for as long as urban society. Ten thousand years ago, the first civilizations in the Fertile Crescent were almost exclusively on earth. Before the industrial revolution, a large portion of the buildings found in European towns were constructed using raw earth methods [10]. In many parts of the world, raw earth construction is common in climates that differ greatly from one another: inland, coastal, plains, mountainous, and hilly regions. One common characteristic is the use of earth that has been collected under the fertile soil layer and is therefore devoid of the organic portion. This earth is made up of silt, sand, and suitable amounts of clay, which serves as a binder. The nearly limitless supply of the construction material, its affordability, and the potential for on-site use without the expense of transportation and transformation have all contributed to the popularity of the earth building technique. Two broad categories can be used to classify the various earth construction methods that have been developed in countless parts of the world based on local conditions: *raw brick*, which uses earth blocks to realize the wall, and *rammed earth*, also known as *pête*, which builds the wall by compacting the earth directly in a box.

Since the blocks may be made off-site, cutting down on drying and installation times and enabling assembly by untrained labor, the method of using raw bricks has attracted renewed attention in the field of self-construction in recent decades [11]. Blocks can be formed using appropriate presses (compressed earth block CEB) or by hand pressing the soil into an open timber frame (adobe). The CEBs approach makes it possible to enhance the block's mechanical properties and prevent erosion during rainy seasons, especially when the soil is stabilized with a small amount of Portland cement (about 6% to 10%). For all of these reasons, the CEBs construction method is suitable for enhancing people's dwelling situations where the economic resources are limited [12,13].

2. State of the art about manually operated presses

To produce Compressed Earth Blocks (CEBs) and Interlocking Stabilized Soil Blocks (ISSBs), hundreds of block presses have been developed since the first machine was invented by the French architect François Cointeraux in 1789. Early historical reviews by Mukerji (1988) [14], Rigassi (1995) [15], and Deboucha and Hashim (2011) [16] trace the technological evolution from traditional hand-tamped adobes to mechanical static compression units. A notable early mobile press was "La Madelon" (Fig. 1 (a)) designed by E. Gossieaux in 1904, which was later improved into "La Super Madelon" (Fig. 1 (b)) and produced by various manufacturers under different names such as "Stabibloc", "Terstaram", and "Ceraman" and utilized until the 1990s. However, these early models were bulky, expensive, and mechanically rigid, which limited their widespread dissemination in self-construction projects.

To address portability and cost limitations, Chilean engineer Raul Ramirez developed the Cinva-Ram in 1952 (Fig. 1 (c)). This system was a lightweight, manually operated press that became one of the most widely adopted block presses worldwide. Despite its widespread success, a fundamental mechanical limitation of the Cinva-Ram and similar manual presses (such as the Bolyn or Hydraform presses reviewed by Ibitoye, 2025 [17]) is that they apply unidirectional compression. Unidirectional pressing creates a pronounced density gradient along the height of the block due to soil-wall friction, resulting in uneven mechanical strength and lower durability.

Recent studies emphasize that achieving high mechanical performance in CEBs requires controlled static compaction pressure (typically between 2 MPa and 5 MPa) at optimum moisture content, as demonstrated by Talibi et al. (2023) [18] and Latha et al. (2023) [19]. To overcome density gradients, bi-directional presses compress two opposing sides of the block simultaneously, significantly improving structural homogeneity. A prominent commercial example of a manual bi-directional press is the Altech Geo50 (Fig. 1 (d)), which has been successfully utilized in humanitarian self-construction programs in Brazil, Argentina, and Senegal [11]. In the Altech Geo50, the operating lever is rigidly attached to a cam, which is connected to the lower mobile frame via a revolute joint. This frame supports the lower pressing plate and undergoes a vertical translation relative to the fixed frame. The follower of the cam mechanism is a roller, connected by a hinge to the upper mobile frame. The block compaction process occurs in two distinct stages. First, the initial rotation of the operating lever drives-via the cam-roller mechanism-the upward vertical translation of the lower plate, executing the first stage of compression from the bottom. Once the lower mobile frame reaches its end-of-stroke limit on the fixed frame, further rotation of the lever induces, through the same cam-roller mechanism, a downward translation of the upper moving frame and its corresponding plate. This subsequent motion compresses the Belleville spring pack interposed between the upper moving frame and the fixed press chassis.

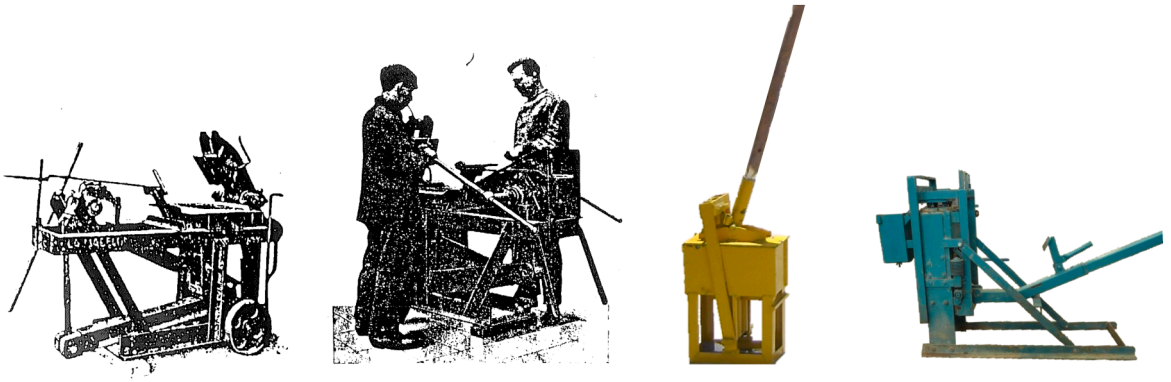


Fig. 1. (a) *La Madelon* (1904) from the product datasheet reported in the appendix of [14]; (b) *La Super Madelon* from the product datasheet reported in the appendix of [14]; (c) *Cinva-Ram* manual brick press; (d) *Altech Geo50* brick press.

2.1. Current bi-directional press limitations

Despite their structural benefits, existing commercial bi-directional presses present critical drawbacks that hinder their adoption in low-resource settings:

1. High structural complexity and elevated fabrication cost: the dual-frame lever of the Altech Geo 50 mechanisms require tight machining tolerances and expensive guidance components;
2. Poor operator ergonomics and safety risks: unassisted lever return and rigid mechanical stops can cause operator fatigue and potential recoil injuries;
3. Non-constant actuation force: because soil compaction exhibits a strongly non-linear exponential resistance curve, traditional linkage/toggle mechanisms demand an extreme, fluctuating input effort from the operator near the end of the stroke;
4. Lack of open-source design optimization: while extensive research exists on soil stabilization mix design (e.g., Zewudie, 2023 [20]; Latha et al., 2023 [18]), there is a clear gap in the literature regarding kinematic optimization for low-cost manual presses.

2.2. Float-Ram novelty and main contributions

To resolve these limitations, the Float-Ram press was introduced. Float-Ram replaces dual moving frames with a single central cylindrical joint and a floating mold, executing bi-directional compression and block ejection through a unified, lightweight chassis. Furthermore, its synthesis uses a custom-designed cam-follower transmission that converts a virtually constant human input effort (300 N) into the exponential compression curve required by the soil, maximizing mechanical efficiency while ensuring operator safety and low production costs. Particular attention in the machine design was devoted to ergonomics and safety. In particular, the machine has been designed to be easy to use with minimum machine reconfigurations and a single input lever. Moreover, the press is designed so that the operator cannot be crushed by the machine's mechanism.

Float-Ram concept was introduced in [21], and in [22]. This paper builds upon Float-Ram concept by providing a description of the local context of the technology application, a detailed presentation of the machine design, an experimental validation on a sensorized prototype of the CEBs press, and the social impact of Float-Ram in several countries around the world.

3. About *Blocco Mattone* compressed earth block

The *Blocco Mattone*, made of pressed and stabilized raw earth (i.e., mixed with a small percentage of cement and/or lime), is the result of experimental research conducted since the 1990s by Prof. Roberto Mattone, a professor of Technology at the Faculty of Architecture of Politecnico di Torino, Italy. The goal of the research was to simplify the production process so that anyone could build high-quality masonry through self-construction. To achieve this goal, Roberto Mattone modified the Altech Geo50 manual press (which initially produced only parallelepiped blocks) to enable the production of a block with protrusions and interlocking joints as shown in Fig. 2. The brick overall dimensions are $140 \times 280 \times 95$ mm. The block has two interlocks in the upper part and two hollows in the bottom part, and a male and female interlocks on the sides (about $1/3$ of the width). These interconnecting geometries help position the blocks in a precise manner, making it easier to build walls, corners, pillars, and other elements of a building. To construct a building with these blocks, a dedicated project is required. The building dimensions must be calculated so that they are multiples of the block size.

In the remainder of this section, the soil selection process and the compressed earth blocks production cycle are presented. A comprehensive description of these topics is out of the scope of this work, but the main procedures and processes are covered to improve the understanding of the entire cycle.

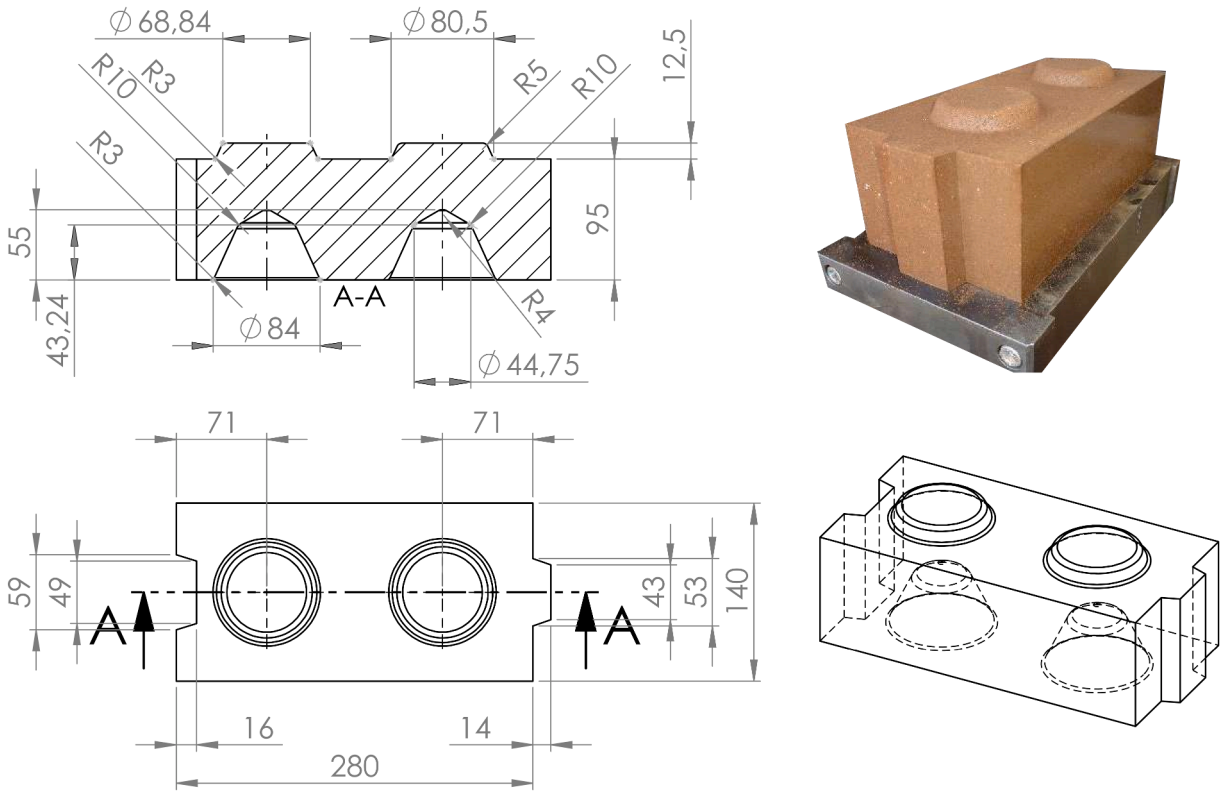


Fig. 2. Technical drawings and dimensions of *Blocco Mattone* in mm.

3.1. Soil selection

The production of blocks made from raw and stabilized soil requires verifying whether suitable soil is available in the area where the project is to be carried out, or whether it can be made suitable by mixing it with sand or other soils.

Engineering-grade bricks require specific soil properties. Given the challenging conditions in which one may find oneself working, so-called "field tests" take on great importance. The following list outlines some of the key tests that can be performed. These recommendations are based on field experience and experimental research tests compiled by the nonprofit organization Mattone su Mattone [11].

1. Visual inspection: assessment of the sandy and fine fractions. Particles smaller than 0.08 mm in diameter are difficult to distinguish with the naked eye
2. Odor test: to assess the presence of organic substances
3. Touch test: determine, with reasonable accuracy, the composition of the soil. Take a sample and remove particles larger than 5 mm in diameter, then rub it between your fingers and the palm of your hand: the presence of sand gives a rough texture; the presence of silt indicates some roughness, but when wet, the soil becomes moderately plastic; the presence of clay, in its dry state, is characterized by grains resistant to breaking, which become plastic when they come into contact with water.
4. Color test: to determine, as a first approximation, the nature of the soil. Gray is associated with calcium carbonates, yellow/ochre to iron hydrates, while red/dark brown to iron oxides.
5. Hand wash test: clay leaves a "soapy" film that is difficult to wash off, whereas with loamy and sandy soils, the hands rinse off easily.
6. Gloss test: take a small ball of slightly damp soil and cut it in half with a knife, clay-rich soil will appear shiny whereas loamy and sandy soils will appear opaque.
7. Sedimentation test: in a 1 L jar put 1/3 L of dry soil and 5/12 L of water, close and shake the jar. The sedimentation layer after 1 min is gravel and sand, after 30 min is gravel, sand, and silt, while after 24 h also clay is sedimented.
8. Dry strength test: high-clay tablets are difficult to break between fingers when dry.
9. Consistency test: roll a 2 cm ball on a table if it is not possible to form a cylinder, clay is absent.
10. Cohesion test: form a 12 mm diameter ribbon and slide it off your palm, measure the length at which the ribbons break. Ideal clay content is associated with lengths in the range 5 cm to 20 cm.

11. Ball drop test: to determine the ideal water content in the mixture. If a 5 cm ball is dropped from 1.1 m, ideal mixture would break into four or five large pieces.
12. Shrinkage test: measure linear contraction in a wooden test mold that is associated with the sand content and granulometry.

3.2. Production cycle

The production process begins with the preparation of the soil, which must be completely dry before processing. Practical field experience dictates sifting the raw soil through a 3 mm mesh sieve to achieve a uniform particle size distribution. If the structural composition requires the addition of sand, it must undergo the same drying and sifting protocol. Next, the dry soil and sand aggregates are dry-mixed with the cement stabilizer(from 6% to 10% in weight) until the matrix achieves a completely homogeneous color.

Water is then introduced gradually while thoroughly agitating the mixture to ensure uniform moisture distribution. Because the hydration process of the cement begins immediately, the stabilized mixture must not be left to rest for more than approximately 60 minutes; consequently, batch sizes should be limited to the production of 15 to 20 blocks at a time. The optimum moisture content of the mix must be verified using the standard drop test (detailed as Test 11 in the preceding section).

Once verified, the mixture is consolidated using the manual press, after which the blocks enter the curing phase. This curing process is critical to the block's final mechanical properties and is executed in three distinct stages:

- Stage 1 (Day 1): The freshly compacted green blocks are placed on a perfectly level surface and completely covered to shield them from direct sunlight and wind, preventing rapid desiccation and cracking.
- Stage 2 (Days 2-3): The blocks begin to gain initial handling strength and must be kept continuously moist through regular water spraying to support the cement hydration.
- Stage 3 (Post-Day 3): The blocks can be safely stacked in two or three rows to optimize space, with moisture maintenance continuing throughout the cycle.

The complete curing profile is concluded, and the blocks reach their nominal characteristic compressive strength, after a standard period of 28 days.

4. Local demands and design requirements

In order to determine whether a technology may be beneficial in a particular setting, it is essential to begin with the wants and concerns of that community and outline the scenario while taking into account the particular living conditions. As a case study, consider Tanzania's Njombe region, where the rural populace primarily engages in small-scale agriculture and the extremely modest homes are constructed using burnt clay bricks and crude methods. These houses are insecure, frequently unhealthy, and not very sturdy.

Typically, the workers fill molds with their bare hands in the mud (as depicted in Fig. 3), which are then flipped over on an open surface to dry in the sun. The bricks are then burned, forming little mounds beneath which the fire is maintained for several days. The bricks generated by this process, example in Fig. 3, are highly uneven, brittle, broken, and inhomogeneous; it also causes deforestation (due to the intensive use of wood) and has a substantial negative environmental impact in the places where it is utilized. Because of the highly uneven shape, building regular-looking walls requires a lot of mortar and, consequently, a lot of concrete between brick courses, and creating decently level walls requires some ability.

In this situation, requests for suitable technologies are generated by local demands, which is a necessary prerequisite for the execution of successful cooperation projects. UN-SDG targets 1.4 and 1.5, which "ensure that all men and women, in particular the poor and the vulnerable, have access to appropriate new technology" and "build the resilience of the poor and those in vulnerable situations and reduce their exposure and vulnerability to climate-related extreme events," respectively, may be affected by appropriate technologies in addition to the previously mentioned SDG11. CEB construction methods are a viable substitute that can improve housing and quality of life, especially in developing nations with rural economies.

4.1. Float-Ram overall design requirements

Float-Ram is designed to address the limitations of existing presses and to produce "Blocco Mattone" type of compressed earth blocks (CEBs) with the geometry defined in Fig. 2. To enhance the quality of the CEBs, the machine should provide bi-directional compression with pressures around 2 MPa.

Given the environmental and social context, manual machines are preferable, as the costs associated with hydraulically operated presses are often unsustainable. Additionally, energy supply can be challenging or even impossible in some regions.

A crucial set of requirements for the design of Float-Ram arises from the CEB production process. As previously described in Section 3.2, the CEB production cycle consists of several key steps. The press is employed during the earth press phase, which can be divided into three main stages: mold filling, block pressing, and block extraction, as illustrated in Fig. 4. Initially, the press is set up for the mold filling operation. The soil mixture is measured using a metering box and then transferred into the mold. It is essential to ensure that the corners of the mold are filled properly with soil; otherwise, the edges of the CEB will not be well-defined after pressing. Next, the machine is reconfigured for the pressing operation, where the earth mixture is compressed bi-directionally. In the final phase, the block is extracted from the press and placed in a controlled environment for curing.



Fig. 3. Comparison of two production methods and resulting bricks: (a) the traditional method for the production of fired bricks, (b) the production method for compressed earth blocks (type "Blocco Mattone") using Float-Ram.

Users should be able to perform all the operations in the most intuitive, safe, and efficient manner. Therefore, the machine must prioritize safety, be easy to use, and allow for straightforward operation. It should execute all tasks with precision and enable quick reconfigurations. Operators should be able to use the machine comfortably, maintaining good posture without needing to exert excessive force.

Additional requirements arise from the conditions of use: the press must be easily transportable on construction sites and able to fit in a pickup vehicle. Additionally, it should feature a "closed" configuration that is compact for effortless shipping to various countries using standard 1200×800 mm pallets and include wheels for limited mobility in operational settings. Keeping costs low is essential while ensuring high quality and reliability.

Finally, to enhance user-friendliness, maintainability, and cost-effectiveness, the machine should be capable of performing the aforementioned phases using a single main kinematic element.

4.2. Experimental soil compression ratio and forces

To perform bi-directional high compression forces on the soil mixture given small operator's forces, Float-Ram will be designed with an force-amplification mechanism. Scientific literature data from [23] had been used to estimate the compression behavior of a standard soil mixture. The data were obtained with cylindrical specimens (diameter 110 mm, initial height h_0 around 150 mm) under static compression. Fig. 5 (a) shows the experimental data of pressure p over the sample height reduction $(h - h_0)$ with different water content w. Water content w can be defined as:

$$w = 100\frac{G_w - G_d}{G_d} \tag{1}$$

where G_w is the weight of the specimen with water, and G_d is the weight of the specimen completely dried.

Among these tests, the intermediate water content $w = 8.5\%$ was selected as the best trade off having a too dry soil mixture (water helps at consolidating the cement uniformly), and minimizing the cracks after the curing phase (too much water in the soil mixture produce cracks during the CEB maturation). Experimental data shows an exponential relationship between volume reduction

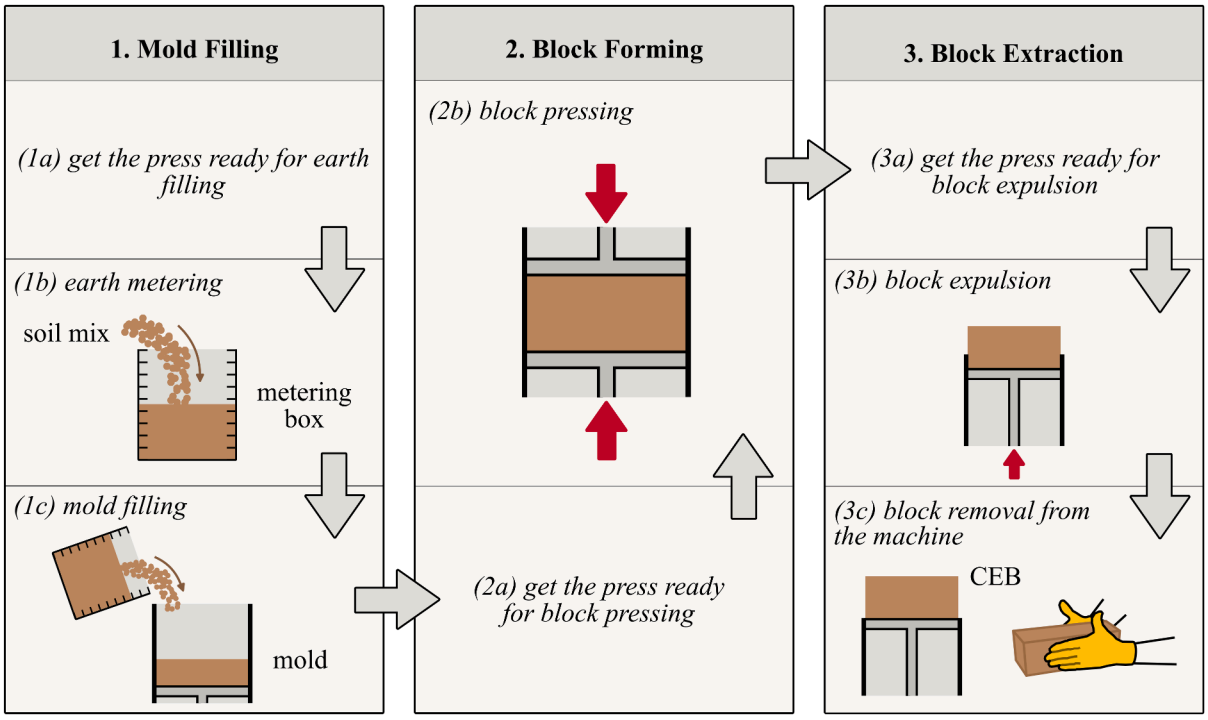


Fig. 4. Earth press stage steps.

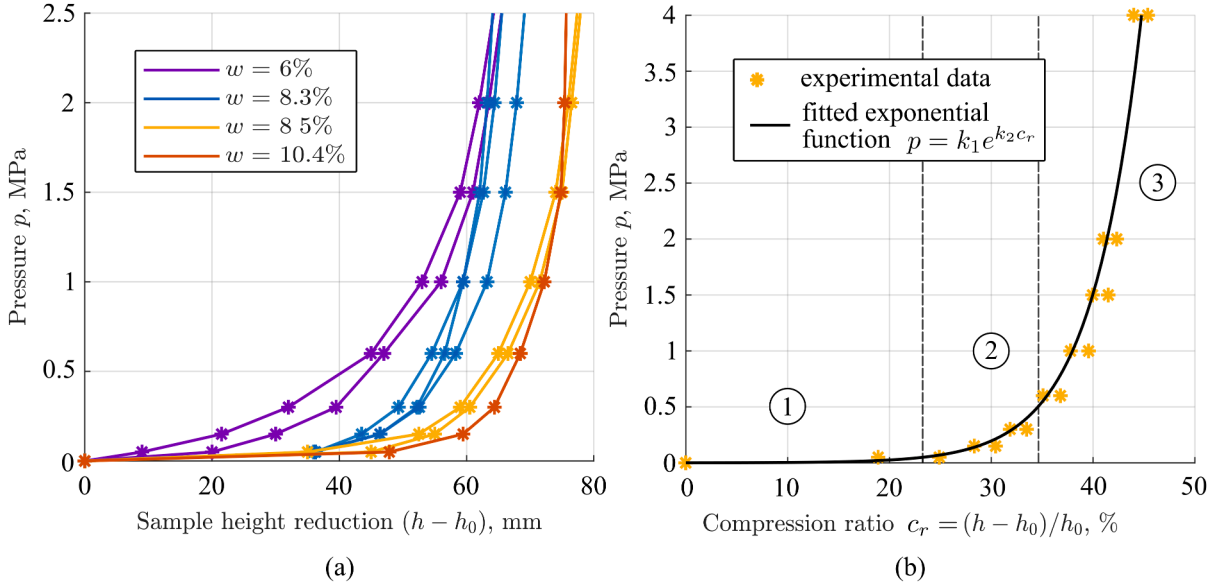


Fig. 5. Earth sample compression tests: (a) pressure p over sample height reduction $(h - h_0)$ with different water content w, given $h_0 = 150$ mm; (b) selected experimental data ($w = 8.5\%$) and exponential fitted function $p = k_1 e^{k_2 c_r}$, where k_1 and k_2 are the exponential coefficients and $c_r = (h - h_0)/h_0$ is the compression ratio reported in the graph as percentage.

percentage and pressure. Fig. 5 (b) shows selected experimental data ($w = 8.5\%$) and exponential fitted function $p = k_1 e^{k_2 c_r}$, where k_1 and k_2 are the exponential coefficients and $c_r = (h - h_0)/h_0$ is the compression ratio reported in the graph as percentage. Numerical values for the exponential coefficients to correlate $c_r = (h - h_0)/h_0$ and p expressed in Pa are $k_1 = 425.7$ Pa and $k_2 = 20.4$.
In literature, it is common to qualitatively divide the compression process in three stages:

1. 0 MPa $\leq p <$ .05 MPa: the air is expelled from the mold;
2. 0.05 MPa $\leq p <$ .5 MPa: the soil grains are pushed together, and the compression starts;

3. 0.5 MPa $\leq p$: compression stage;

From this exponential function it is possible to estimate the initial height needed to get compression pressures around 2 MPa with a fixed final block height as in Fig. 2. In particular, a compression pressure of 2 MPa is associated with a compression ratio $c_r = 41.7\%$. Therefore, to have a final block of height of 95 mm, the initial block height must be 163 mm, with a compression stroke of 68 mm. This exponential function will be also used to design the cam profile in Section 5.2.

5. Machine design

5.1. Machine overview

To address all the requirements presented in Section 4, the machine is conceived with the following important design features (Fig. 6):

1. the machine is designed around a central cylindrical kinematic pair that enables all the block pressing phases with a fast, safe and ergonomic reconfiguration among the earth-filling phase, the block-pressing phase, and the block-expulsion phase. A single input lever is used to apply the compression and expulsion input forces and to shift from one configuration to the following one. The machine is designed to perform all the required operations with a maximum input lever rotation of 90° for the compression and expulsion phases;
2. bi-directional compression is obtained using a floating-mold, i.e., the compression force is provided through the bottom plate of the mold to the earth, the mold ceiling is fixed to the frame, while the sides are free to move vertically. This feature enable bi-directional compression without complex mechanisms that actuate both the mold ceiling and bottom simultaneously;
3. a cam-follower transmission system is used to convert the rotation of the input lever into the translation of the mold bottom plate. The cam profile is designed to obtain the 2.0 MPa of compression pressure of the soil starting from a quasi-constant input force around 300 N applied by the operator on the input lever at the end of the lever. The cam synthesis process is detailed in Section 5.2;
4. a second cam-follower transmission is used to extract the block from the press, after the block-pressing phase;
5. a compression spring supports the weight of the float mold and the cam-assembly and the preload is tuned in such a way that the floating mold can be positioned under the ceiling with a few milliliter gap. When the user put the cam in contact with the roller, part of the weight is transferred from the spring to the roller and the floating mold lifts slightly closing the gap and ensuring that the floating mold is aligned with the ceiling. Once everything is ready, the compression phase can start;
6. the press is foldable for easy transportation and storage, and it has wheels for small movements at the construction site;
7. a metering box with adjustable bottom is placed next to the mold in the earth-filling phase, and it is used to fill the mold with the same amount of earth every time.

The selection of a custom cam-follower mechanism over other traditional mechanical linkage chains (e.g., four-bar linkages, toggle mechanisms, or rack-and-pinion drives) is driven by the strongly non-linear compaction behavior of soil mixtures. As established in Section4.2, soil compaction exhibits an exponential resistance profile $p = k_1 e^{k_2 c_r}$, where compression resistance rises sharply from near-zero to 2.0 MPa over a limited bottom-plate displacement. Standard linkage mechanisms possess fixed mechanical advantage profiles governed by the geometric link ratios and selected range of motion. For example, toggle mechanisms provide high force amplification only near the singular toggle point over a very narrow displacement range, resulting in uneven operator effort and severe force spikes. In contrast, a cam mechanism allows point-by-point analytical synthesis of the transmission ratio function. This capability allows the machine to precisely invert the exponential soil reaction curve, mapping it into a virtually constant human input effort (≈ 300 N) across the entire lever rotation.

Fig. 6 illustrates the main components and CEB production phases. First, the mold is positioned in the mold filling configuration (phase *(1a)*) and the metering box is filled with the soil mixture (phase *(1b)*). Preliminary tests must be conducted to set the correct amount of earth for optimal results since each type of soil has specific properties. The metering box has an adjustable bottom to regulate the amount of soil mixture to be transferred to the next phase. Then, the metering box is rapidly rotated to transfer the earth into the mold (phase *(1c)*).

At this point, the operator uses the input lever to rotate the floating mold and cam assembly around the cylindrical pair shaft, placing the floating mold under the mold ceiling (phase *(2a)*). In this way, the machine is in the block pressing configuration as in Fig. 6 (b). During the machine reconfiguration the weight of the mold, cam assembly, and soil mixture is supported by an axial bearing mounted on the cylindrical pair shaft, requiring low physical effort from the operator. The cam assembly weight is supported by four end-stop pins at the bottom of the floating mold, while the floating mold cylindrical pair is resting on top of a compression spring that is placed on top of the axial bearing. The compression spring is regulated to leave a very little gap (around 1 mm) under the weight of the floating mold, cam assembly, and soil mixture between the floating mold and the mold ceiling. This is a safety feature to be sure that nothing is trapped between the floating mold and the mold ceiling before the compression forces are applied.

When the machine is in the block pressing operation, the compression cam (green cam in Fig. 6) is in contact with the compression roller, a passive roller hinged to the frame defined in Fig. 6 (a). Then, the operator lowers the lever (as illustrated in Fig. 6 (c)) by applying the input force. Since the cam support is jointed to the shaft through a cylindrical pair, the revolute joint connecting the cams to the cam support moves vertically and so does the mold bottom plate. Contrary to usual schemes, the cam axis is free to translate and rotate, while the roller has a rotation axis in a fixed position with respect to the frame. During the compression phase (phase

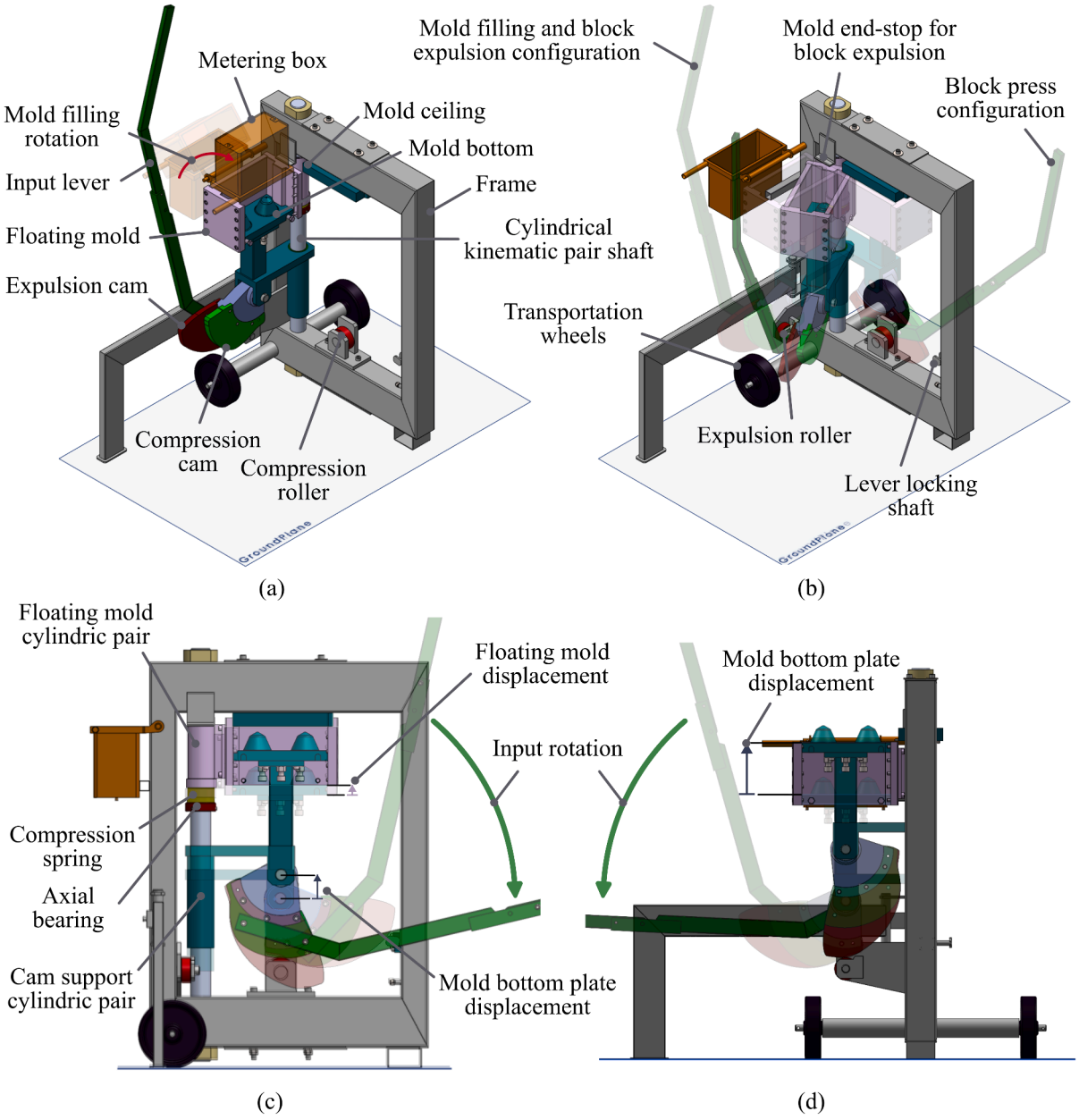


Fig. 6. Float-Ram mechanical architecture and operational phases: (a) mold filling phase; (b) machine reconfiguration; (c) block press phase; (d) block expulsion phase.

(2b)), the bottom plate applies compression forces to the soil mixture, the soil compresses, and the floating mold moves vertically because of the friction forces between the soil and the floating mold, obtaining a bi-directional compression of the block.

Given the compression cam profile, whose design is detailed in Section 5.2, when the operator completes the input lever rotation, the compression pressure depends on the amount of soil that was placed inside the mold. To ensure that the final compression pressure is around 2.0 MPa, the operator must apply an input force around the design value 300 N. If the perceived force is smaller than the design value, the block at the end of the compression phase will have the correct geometry, but insufficient compaction, so it must be discarded. If, otherwise, the forces are higher, it is recommended to stop the compression in order not to damage the machine.

Then, the input lever is raised and the press is configured for the expulsion of the block (phase *(3a)*) by rotating the floating mold, cam-assembly and soil mixture around the main shaft. In this configuration the expulsion cam (red cam) is resting on top of the expulsion roller (defined in Fig. 6 (a) and (b)). The operator lowers the input lever to extract the block from the mold (phase *(3b)*). The rotation of the input lever is converted into a vertical displacement of the mold bottom plate through the expulsion cam-follower

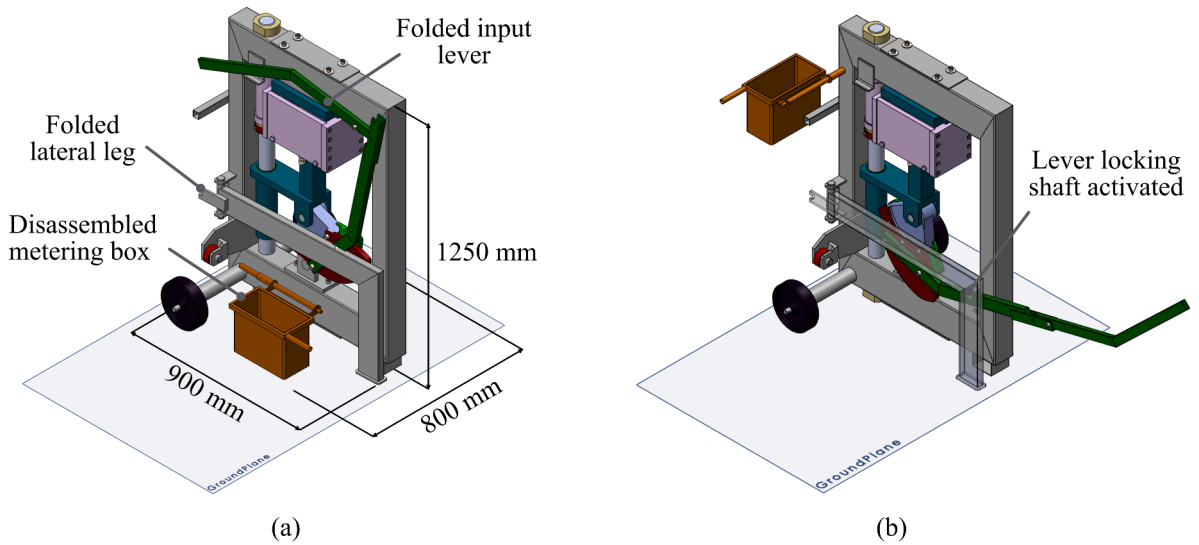


Fig. 7. Float-Ram additional details: (a) shipping configuration; (b) input lever locked for easy movements at the construction site.

systems. It should be underlined that in this phase the floating mold cannot move vertically because of a mold end-stop fixed to the frame (as illustrated in Fig. 6 (b)). Finally, the operator extracts the block from the press and placed it in a controlled environment for curing (phase *(3c)*).

Additional details are provided in Fig. 7. In Fig. 7 (a), the machine is represented in the shipping configuration: the metering box is disassembled and the lateral leg and input lever are folded. In the shipping configuration the overall dimensions are $800 \times 900 \times 1250$ mm. In Fig. 7 (b), Float-Ram is shown with the input lever locked by the lever-locking shaft. In this configuration, the input lever can be used to raise the machine on the wheels for small movements at the construction site.

5.2. Compression cam synthesis

The design of the cam system is a fundamental aspect to ensure ergonomic conditions for the operator. Fig. 8 presents a functional scheme of the cam-transmission for the block pressing operation. In this section, the design process of the compression cam profile is presented in a general case to be easy replicated. The numerical values used in the design of the compression cam are summarized in Table 1 at the end of the section. The following graphs depict the actual trends of the variables in the final cam design, but are presented in a generalized manner using the symbols illustrated below.

First, some important definitions: p is the pressure acting on the block surface A; $F = pA$ is the resulting compression force acting on the block; $T = l_u F_u$ is the operator torque provided by the user that is applying a force F_u on the input lever at a normal distance l_u from the O_1 axis; y is the stroke of the mold bottom plate; z the stroke of the floating mold; α is the input lever rotation. Since multiple reference frames are used for the definition of the cam motion law $y(\alpha)$, three subscripts are defined: l indicates the variables with respect to (wrt) the beginning the lift motion of the mold bottom plate, c indicates the variables wrt the beginning of the compression phase, f indicates the variables wrt the beginning of final deceleration phase after the compression. For example, $y_c = 10$ mm describes a mold bottom displacement of 10 mm from the beginning of the compression phase.

Fig. 8 (c) defines important geometric parameters of the machine: q is the height of the block (q_0 after the mold filling operation and before the block pressing and q_f after the block pressing phase), t is the total aperture of the machine frame from O_2 axis to the mold ceiling, g is the design gap between the cam in the initial position and the passive compression roller (radius R_r), d is the gap between the top of the mold ceiling and the top surface of the soil mixture, R_{b0} is the prime circle radius of the cam profile, and b is the distance between the O_1 axis and the mold bottom plate upper surface.

The cam profile was designed starting from the experimental identification of the pressure trend during the compression of the block as presented in Section 4.2. The selected experimental compression trend presented in Fig. 5 (b), can be adapted to the "Blocco Mattone" dimensions to the get the trend of the pressure over the stroke of the mold bottom plate as shown in Fig. 9 (a). Considering the block area A, the resulting force required for the compression in presented in Fig. 9 (b) as a black dashed line (pA in the legend).

At this stage, it is useful to introduce minor adjustment to the force profile. In fact, in the first part of the compression, it is useful to have a non zero initial force because the operator input torque T needs to compensate the friction forces within the system. For this reason, a polynomial function is introduced for $0 \le y_c < y_{CI}$. After the polynomial section, the synthesis of the cam profile will follow the exponential force profile in the range $y_{CI} \le y_c \le y_{CII}$. Therefore, the force profile is described by the function:

$$F = F(y_c) = \begin{cases} F_0 + c_n y_c^n & 0 \le y_c < y_{CI} \\ c_1 e^{c_2 y_c} & y_{CI} \le y_c \le y_{CII} \end{cases} \tag{2}$$

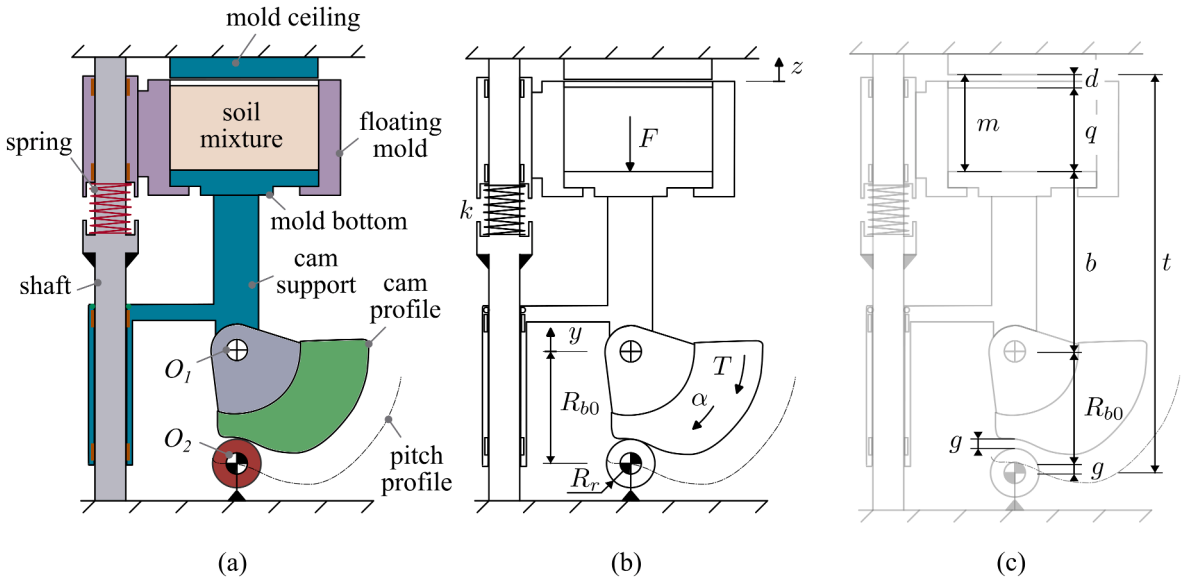


Fig. 8. Float-Ram scheme of the cam-transmission for the block press phase: (a) scheme with components definition; (b) variables and parameters definition; (c) definition of the geometric parameters regarding clearance.

The coefficients of the polynomial section c_n and n can be evaluated by imposing the continuity of F and its first derivative dF/dy_c at $y_c = y_{cI}$:

$$F_I = F(y_{cI}) = F_0 + c_n y_{cI}^n \quad \Rightarrow \quad c_n = \frac{F_I - F_0}{y_{cI}^n} \tag{3}$$

$$\frac{d}{dy_c} F(y_{cI}) = c_n n\, y_{cI}^{n-1} = \frac{F_I - F_0}{y_{cI}^n}\, n\, y_{cI} = n\frac{F_I - F_0}{y_{cI}} = c_1 c_2\, e^{c_2 y_{cI}} \quad \Rightarrow \quad n = \frac{c_1 c_2}{F_I - F_0}\, y_{cI}\, e^{c_2 y_{cI}} \tag{4}$$

The efficiency η of the transmission is equal to the ratio between the compression work W on the block and the work W_u done by the user:

$$\eta = \frac{dW}{dW_u} = \frac{F\,dy}{T\,d\alpha} \tag{5}$$

The compression work W can be evaluated as a function of the vertical displacement of the mold bottom plate during the compression phase as:

$$W = W(y_c) = \begin{cases} \int_0^{y_c} (F_0 + c_n y_c^n)\, dy_c = F_0 y_c + \frac{c_n}{n+1} y_c^{n+1}; & 0 \le y_c \le y_{cI} \\ \int_0^{y_{cI}} (F_0 + c_n y_c^n)\, dy_c + \int_{y_{cI}}^{y_c} (c_1 e^{c_2 y_c})\, dy_c = W_I + \frac{c_1}{c_2}(e^{c_2 y_c} - e^{c_2 y_{cI}}); & y_{cI} < y_c \le y_{cII} \end{cases} \tag{6}$$

where $W_I = W(y_{cI}) = F_0 y_{cI} + \frac{c_n}{n+1} y_{cI}^{n+1}$ is the compression work at the end of the polynomial section.

Because the Float-Ram press is manually operated at low actuation speeds, the inertial forces and dynamic accelerations of the moving components are negligible compared to the magnitude of the soil compaction forces. Consequently, while dynamic inertial effects are negligible, the machine's kinetostatic model (quasi-static force equilibrium at each angular position α) is needed to define the instantaneous transmission ratio $y'(\alpha)$ necessary to transform the exponential soil compaction resistance into a nearly constant operator effort (≈ 300 N) throughout the entire lever stroke.

Given a desired constant input torque T, the work W_u performed by the user is $W_u = W_u(\alpha_c) = T\alpha_c$. If $\eta = 1$ is assumed, the relationship between the input angle α_c and the vertical displacement of the mold bottom plate during the compression phase y_c can be evaluated as:

$$\alpha_c = \alpha_c(y_c) = \frac{1}{T} W(y_c) = \frac{1}{T} \begin{cases} F_0 y_c + \frac{c_n}{n+1} y_c^{n+1}; & 0 \le y_c \le y_{cI} \\ W_I + \frac{c_1}{c_2}(e^{c_2 y_c} - e^{c_2 y_{cI}}); & y_{cI} < y_c \le y_{cII} \end{cases} \tag{7}$$

In this way, the cam profile in the compression section is completely defined. The motion law $y_c = y_c(\alpha_c)$ is the inverse function of the one presented in (7). Fig. 10 (a) presents the compression work as a function of y_c, Fig. 10 (b) the work done by the operator during compression as a function of the cam rotation α_c, while Fig. 10 (c) and (d) illustrate the relationship between the mold bottom displacement y_c and the cam rotation α_c.

Because of the gaps g and d present in the systems, the compression phase does not start as soon as the operator rotates the input lever. Therefore, to consider this approach phase, an initial phase must be added before the compression starts. As presented before,

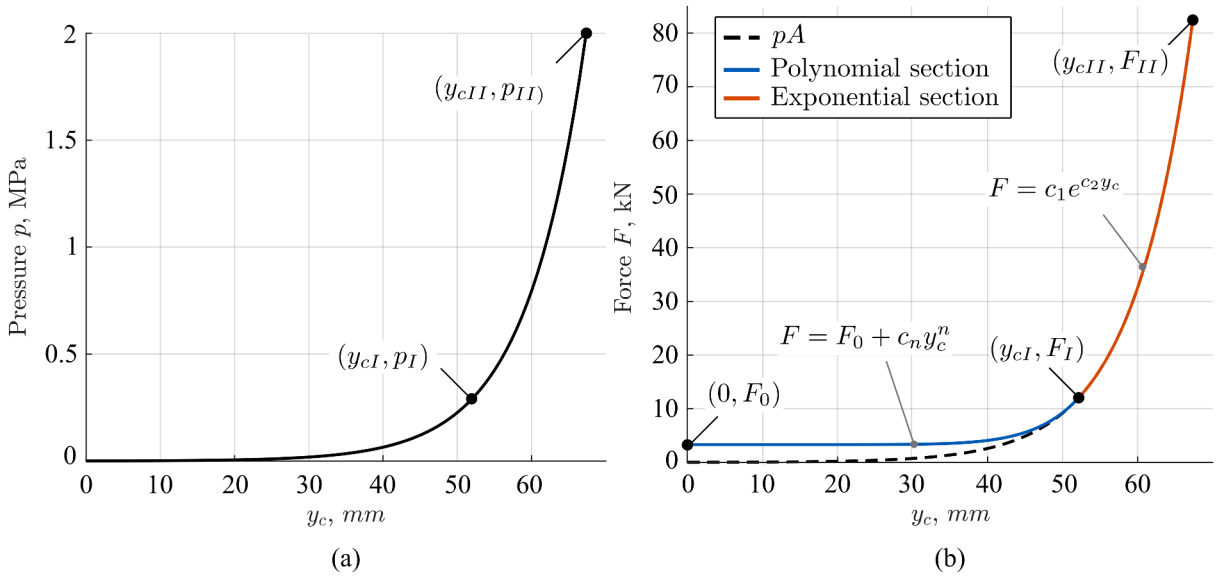


Fig. 9. (a) pressure trend over the mold bottom plate displacement during compression; (b) force profile over the mold bottom plate displacement during compression.

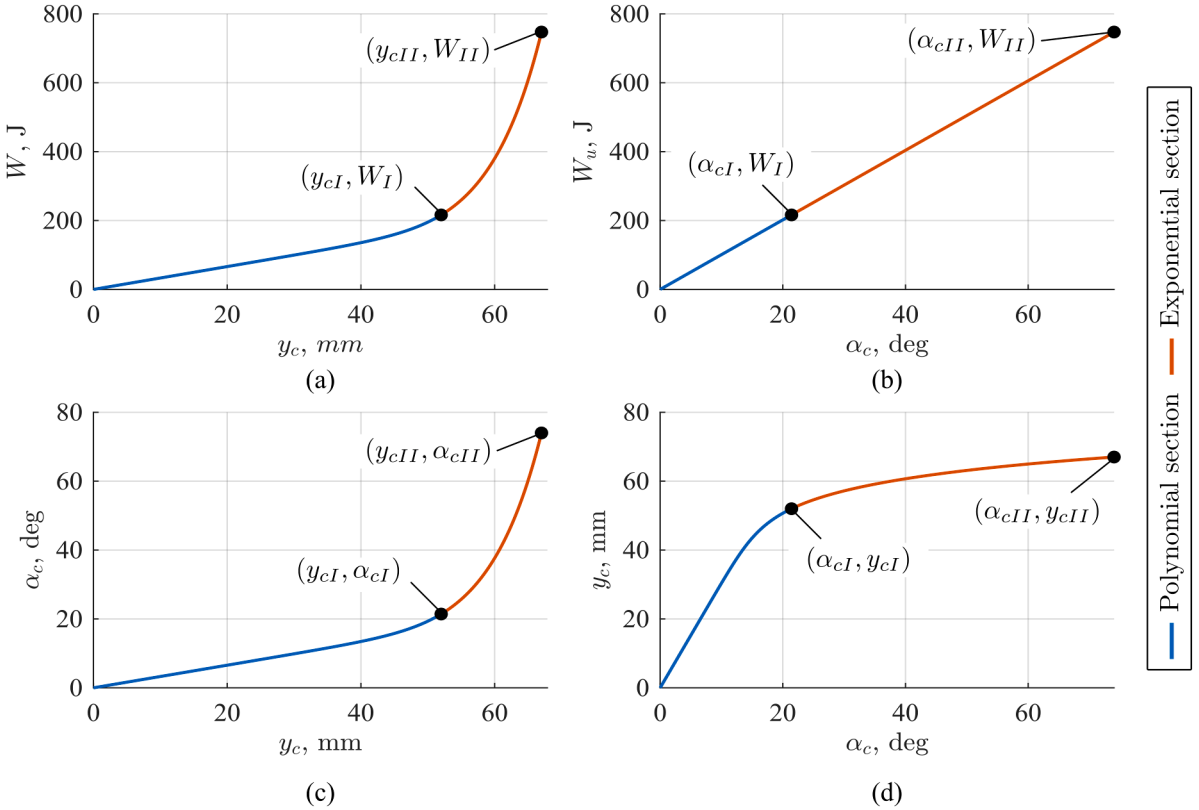


Fig. 10. (a) compression work over the mold bottom plate displacement; (b) work done by the operator during compression over the cam rotation; (c) angular rotation over the mold bottom plate displacement; (d) motion law of the cam during compression.

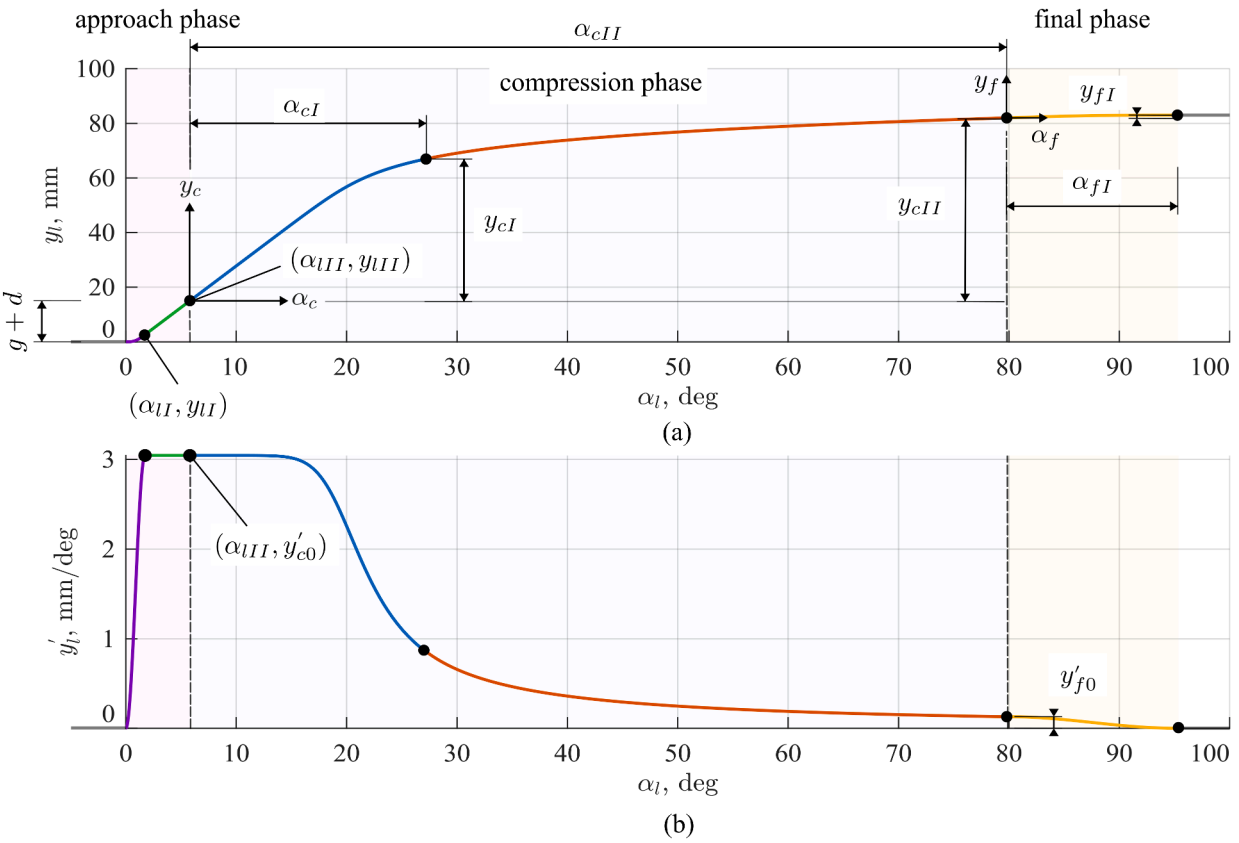


Fig. 11. (a) mold bottom plate motion law y as a function of the cam rotation α wrt the beginning of the mold bottom plate vertical displacement (reference frame identified with the subscript l); (b) geometric velocity $y'_l = dy_l/d\alpha_l$ as a function of the cam rotation α_l.

the subscript l describes the variables wrt the beginning the lift motion of the mold bottom plate. During this phase, the mold bottom plate moves vertically of $y_{lII} = g + d$, while the cam rotates of α_{lII}, as shown in Fig. 11. Since the total gap $g + d$ may vary during the CEBs production, it is useful to design this approach phase in two sections. The first section (purple section in Fig. 11) connects the cam profile at constant curvature radius $(R_{b0} - R_r)$ to a second part of the cam profile (green section in Fig. 11) with a linear relationship between y and α with proportional coefficient equal to $y'_{c0} = dy_c(\alpha_c = 0)/d\alpha_c$. In this way, even if the compression phase starts at $\alpha_l = \alpha_{lII} \pm \delta_l$, where δ_l is a small error in the angular cam rotation, the operator will perceive the same transmission ratio y'_{c0}. Thus, the motion law during the approach phase can be written as:

$$y_l = \begin{cases} \frac{y_{lI}}{\alpha_{lI}}\alpha_l - \frac{y_{lI}}{\pi}\sin\left(\frac{\pi}{\alpha_{lI}}\alpha_l\right) & 0 \le \alpha_l < \alpha_I \\ y'_{c0}\alpha_l + (y_{lII} - y'_{c0}\alpha_{lII}) & \alpha_I \le \alpha_l < \alpha_{II} \end{cases} \tag{8}$$

A design parameter $k_l = \alpha_{lI}/\alpha_{lII}$ can be introduce to relate α_{lI} and α_{lII}. In this way, since $y_{lII} = g + d$, the unknown parameters α_{lII} and y_{lI} can be evaluated by imposing the continuity of the function $y_l = y_l(\alpha_l)$ and its first derivative $y'_l = y'_l(\alpha_l)$ at $\alpha_l = \alpha_{lI}$:

$$y'_l(\alpha_{lI}) = y'_{c0} \quad \Rightarrow \quad y_{lI} = y'_{c0}\frac{k_l\,\alpha_{lII}}{2} \tag{9}$$

$$y_l(\alpha_{lI}) = y_{lI} \quad \Rightarrow \quad \alpha_{lII} = \frac{y_{lII}}{y'_{c0}(1 - k_l/2)} \tag{10}$$

Finally, a deceleration stage is added after the compression to let the operator perceive the end of the compression phase. To do so, a transition cam profile is introduce to connect the end of the compression section to a part of the cam with constant curvature radius. Given a constant curvature radius, it is expected that the operator will perceive a zero-resistance zone that indicates the end of the compression phase. If y'_{f0} is the first derivative of the motion law at the end of the compression phase, the motion law in the final section can be written as:

$$y_f = \frac{y'_{f0}}{2}\left(\frac{\alpha_{fI}}{\pi}\sin\left(\frac{\pi}{\alpha_{fI}}\alpha_f\right) + \alpha_f\right) \tag{11}$$

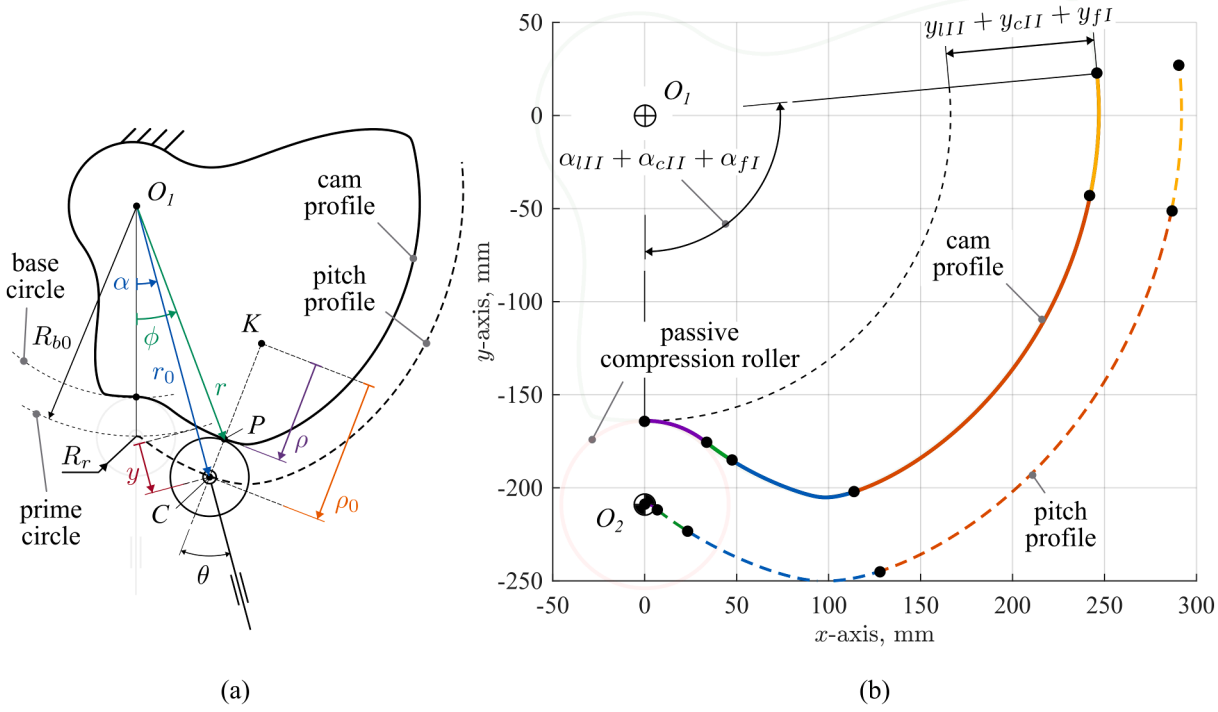


Fig. 12. (a) cam synthesis variables definition; (b) compression cam profile after the synthesis process.

where $\alpha_{fI} = 2y_{fI}/y'_{f0}$, and y_{fI} is a design parameter that can be used to tune the deceleration phase.

Given the overall motion law shown in Fig. 11, the cam profile can be obtained using standard methods for cam synthesis (analytical or graphical methods). Since these methods are well known in the field, only the main results of analytical cam synthesis are reported in the following part of this section [24]. The synthesis procedure starts with the kinematic inversion, i.e., the cam is considered fixed and the frame rotates of $-\alpha$, as illustrated in Fig. 12 (a). The pitch curve and the cam profile will be described using polar coordinates, respectively (r_0, α) and (r, ϕ). For all α, the position of the axis O_2 on the pitch curve is C, while the roller contacts the cam profile in P, and K is the curvature radius center of the cam profile.

The pitch profile can be evaluated from the total motion law $y(\alpha)$ in Fig. 11 as $r(\alpha) = R_{b0} + y(\alpha)$. The cam pressure angle θ can be evaluated as:

$$\theta = \theta(\alpha) = \operatorname{atan}\left(\frac{y'(\theta)}{r(\alpha)}\right) = \operatorname{atan}\left(\frac{y'(\theta)}{R_{b0} + y(\theta)}\right); \quad \text{where } y' = \frac{dy}{d\alpha} \tag{12}$$

The pitch curve curvature radius ρ_0 and the cam profile curvature radius ρ can be evaluated as:

$$\rho_0 = \rho_0(\alpha) = \frac{\left(r_0^2 + y'^2\right)^{3/2}}{y'(3r_0 - y'')}; \qquad \rho = \rho_0 + R_r; \quad \text{where } y'' = \frac{d^2y}{d\alpha^2} \tag{13}$$

Finally, the cam profile polar coordinates can be evaluated as:

$$r = r(\alpha) = \sqrt{R_r^2 + r_0^2 - 2R_r r_0 \cos(\theta)}; \qquad \phi = \phi(\alpha) = \alpha + \operatorname{asin}\left(\frac{R_r}{r}\sin(\theta)\right) \tag{14}$$

Fig. 12 (b) shows the resulting cam profile after the synthesis process, with the sections of the profile identified using the same colors as in Fig. 11: the purple section is the first part of the approach phase, the green section is the second part of the approach phase, the blue and orange sections are the compression phase (polynomial and exponential section), while the yellow part the deceleration phase. Fig. 12 (b) presents the relevant part of the compression cam profile. For convenience it is useful to add dwell sections at the beginning and at the end of the cam, while the remaining of the profile doesn't have functional requirements and can be designed to reduce the weight.

5.3. Expulsion cam synthesis

This section presents briefly the expulsion cam synthesis. Contrary to the compression phase where the main design requirement is given by the compression behavior of the earth, the expulsion cam design requirements are only based on the total rotation of the input lever α_{em} (where the subscript e indicates the expulsion phase, while m indicates the maximum value of α_e), and the total vertical displacement y_e of the mold bottom plate that is required to lift the CEB outside the mold.

Table 1
Float-Ram compression cam design parameters and dimensions.

Description	Symbol	Value
Compressed Earth Block (CEB) area	A	39200 mm^2
Height of the CEB before the block pressing	q_0	163 mm
Height of the CEB after the block pressing	q_f	95 mm
Passive roller radius	R_r	45 mm
Base radius of the cam profile	R_{b0}	209 mm
Pressure on the CEB at the end of the polynomial section	p_I	0.3 MPa
Pressure on the CEB at the end of the exponential section	p_{II}	2.0 MPa
Initial force of the modified force profile	F_0	28% F_I = 3318 N
Exponential section coefficient	c_1	16.50 N
Exponential section coefficient	c_2	126.47 m^{-1}
Mold bottom plate displacement at the end of the polynomial section	y_{cI}	52 mm
Mold bottom plate displacement at the end of the exponential section	y_{cII}	67 mm
Cam angular rotation at the end of the polynomial section	α_{cI}	21.4°
Cam angular rotation at the end of the exponential section	α_{cII}	74°
Design gap between the cam and the passive roller	g	5 mm
Initial gap between the mold ceiling and the earth surface	d	10 mm
Ratio between α_{fI} and α_{fII}	k_f	30%
Mold bottom plate vertical displacement during the final section	y_{fI}	1 mm

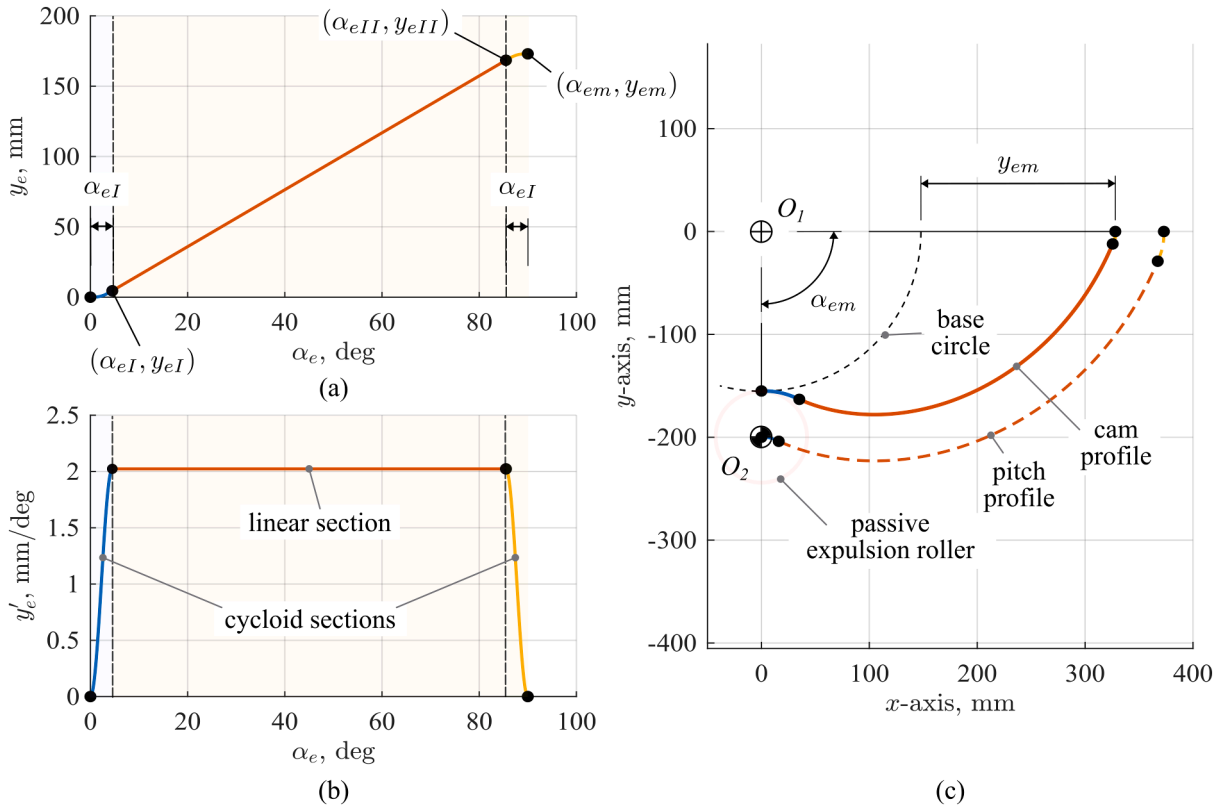


Fig. 13. Expulsion cam synthesis: (a) motion law $y_e(\alpha_e)$; (b) transmission ratio $y'_e(\alpha_e)$; (c) expulsion cam profile after the synthesis process.

Many types of motion law $y_e(\alpha_e)$ can be adopted to design the expulsion cam. In this case, the adopted motion law is a symmetric function characterized by three parts: the first and third parts are cycloid motion laws, while the second part is a linear motion law as depicted in Fig. 13 (a) and (b). The motion law is defined by:

$$y_e = \begin{cases} \frac{y_{eI}}{\alpha_{eI}}\alpha_e - \frac{y_{eI}}{\pi}\sin\left(\frac{\pi}{\alpha_{eI}}\alpha_e\right) & 0 \le \alpha_e < \alpha_{eI} \\ 2\frac{y_{eI}}{\alpha_{eI}}(\alpha_e - \alpha_{eI}) + y_{eI} & \alpha_{eI} \le \alpha_e < \alpha_{eII} = \alpha_{em} - \alpha_{eI} \\ y_{eII} + \frac{y_{eI}}{\alpha_{eI}}(\alpha_e - \alpha_{eII}) + \frac{y_{eI}}{\pi}\sin\left(\frac{\pi}{\alpha_{eI}}(\alpha_e - \alpha_{eII})\right) & \alpha_{eII} \le \alpha_e \le \alpha_{em} \end{cases} \quad (15)$$

where $y_{eI} = y_e(\alpha_{eI}) = \frac{y_{em}}{2(k_e-1)}$, $k_e = \alpha_{em}/\alpha_{eI}$, and $y_{eII} = y_e(\alpha_{eII}) = 2\frac{y_{eI}}{\alpha_{eI}}(\alpha_{eII} - \alpha_{eI}) + y_{eI}$.

The design requirements are $\alpha_{em} = \pi/2$ and $y_{em} = q_0 + d$, while the design parameter k_e can be used to tune how long the initial and final cycloid section are with respect to the total cam rotation α_{em}. Using the same analytic synthesis process described in the previous section, the resulting expulsion cam profile is shown in Fig. 13 (c).

5.4. Float-Ram prototype

Fig. 14 illustrates the machine prototype. In Fig. 14 (a), Float-Ram is shown in the shipping configuration, with the metering box disassembled, the lateral leg closed and the input lever folded. Fig. 14 (c)–(e) illustrate the mold filling operation: first the metering box is filled with the soil mixture, then the metering box is rotated and the soil is manually pre-compressed in the corners to ensure crisp edges in the final CEB. Then, the machine is re-configured in the compression configuration (Fig. 14 (b)), and the compression is achieved by rotating the input lever (Fig. 14 (f) and (g)). After the compression, the machine is configured again (Fig. 14 (h)) for the CEB expulsion (Fig. 14 (i) and (j)). Finally, the CEB is removed from the machine and transferred in a controlled environment for curing.

The machine's frame is made from rectangular-section structural steel profiles that are cut and welded together to form the portal frame. The same manufacturing process is used for the lateral leg and the input lever. The metering box is made of structural steel sheets folded and welded together. The cylindrical joint shaft is made of ground and chrome-plated special steel, the same material used for the hydraulic pistons used in earthmoving equipment. On the sliding support components (cam support and floating mold support in Fig. 6), gasket for pistons are installed to keep the dirt out of the axial and radial bushings that are filled with bearing grease. The mold lateral plates, bottom and ceiling are made of carburized and nitrided special steel to improve wear resistance. The compression and expulsion rollers are commercial components produced by SKF (model NUTR 4090).

The spring that supports the floating mold is made of Inox for springs, and it has custom parameters: wire diameter 8 mm, mean spring diameter 72 mm, external diameter 80 mm, internal diameter 64 mm, minimum loaded spring length 30 mm, unloaded spring length 75 mm, four active coils and one non-active and machined coil at each end.

The wheels for small movements at the construction site have a solid rubber, external diameter 200 mm, shaft diameter 20 mm, and width 50 mm.

The entire project is available open-source on GitHub. The CAD model of the Float-Ram is available both in STEP and SOLIDWORKS (2024) format, and a detailed component list is provided with part numbers and specifications. Additionally, the open-source project will provides information on how to build and use a custom testing apparatus to test the bending resistance of seasoned CEBs. Then, empirical formulas can be used to estimate the compressive strength of the block.

6. Experimental tests

To test the effectiveness of the machine during the compression phase, an instrumented version has been tested in the laboratory. The experimental setup is illustrated in Fig. 15. Two linear transducers are used to measure the linear displacement of the mold bottom plate y and of the floating mold z. Then, an angular transducer is installed between the cam carrier and the cam assembly to measure the input rotation α. Finally, two load cells are used to measure the input force F_{cable} and the output force F. The input force is provided using an inextensible cable connected to the input lever at point A. The input cable wraps around a passive pulley, and B_0 is the tangency point between the cable and the passive pulley at the initial condition. Since only very small variations occur during the compression phase, the tangency point is considered constant and equal to B_0. The initial condition is completely defined by the geometric distances: $a_0 = \text{const.} = 1515$ mm, $c_0 = \text{const.} = 1785$ mm, $e_0 = e(\alpha = 0) = 2445$ mm, $f_0 = f(\alpha = 0) = 1510$ mm. Using the following equation, it is possible to convert the measured cable tension F_{cable} into the force applied by the user F_u used in the design phase.

$$\delta_0 = \delta(\alpha = 0) = \operatorname{asin}\left(\frac{f_0}{a_0}\right); \quad \psi_0 = \psi(\alpha = 0) = \frac{\pi}{2} - \delta_0; \quad \epsilon_0 = \text{const.} = \operatorname{acos}\left(\frac{a_0^2 + c_0^2 - e_0^2}{2a_0c_0}\right) - \delta_0 \tag{16}$$

$$B_0 = B_{0,x}\hat{\imath} + B_{0,y}\hat{\jmath} = c_0\begin{bmatrix}\cos(\epsilon_0)\\ -\sin(\epsilon_0)\end{bmatrix}; \qquad A = A_x\hat{\imath} + A_y\hat{\jmath} = \begin{bmatrix}a_0\sin(\theta_0 + \alpha)\\ a_0\cos(\theta_0 + \alpha)) + y(\alpha)\end{bmatrix}; \tag{17}$$

$$\beta = \sqrt{(x_A - x_{B_0})^2 + (y_A - y_{B_0})^2}; \quad \Rightarrow \quad n = a_0\sin(\beta) \tag{18}$$

$$T = nF_{cable}; \qquad F_u = \frac{T}{a_0} = \frac{nF_{cable}}{a_0} \tag{19}$$

Multiple tests were conducted to evaluate the machine's performance with varying soil quantities in the mold. Specifically, the test has been repeated with six different amounts of soil with masses in the range from 6.8 kg to 7.3 kg.

The experimental results are shown in Fig. 16. As expected, varying the soil quantity alters the required compaction force F: a higher volume of earth correlates with a higher compression force F since more material need to be compressed. Due to the mechanical advantage provided by the cam-follower transmission ratio, these compression forces map back to the input user forces



Fig. 14. Float-Ram: (a) shipping configuration, (b) compression configuration, (c) metering box filling, (d) and (e) mold filling, (f) and (g) compression phase, (h) machine re-configuration, (i) and (j) expulsion phase, (k) CEB transfer.

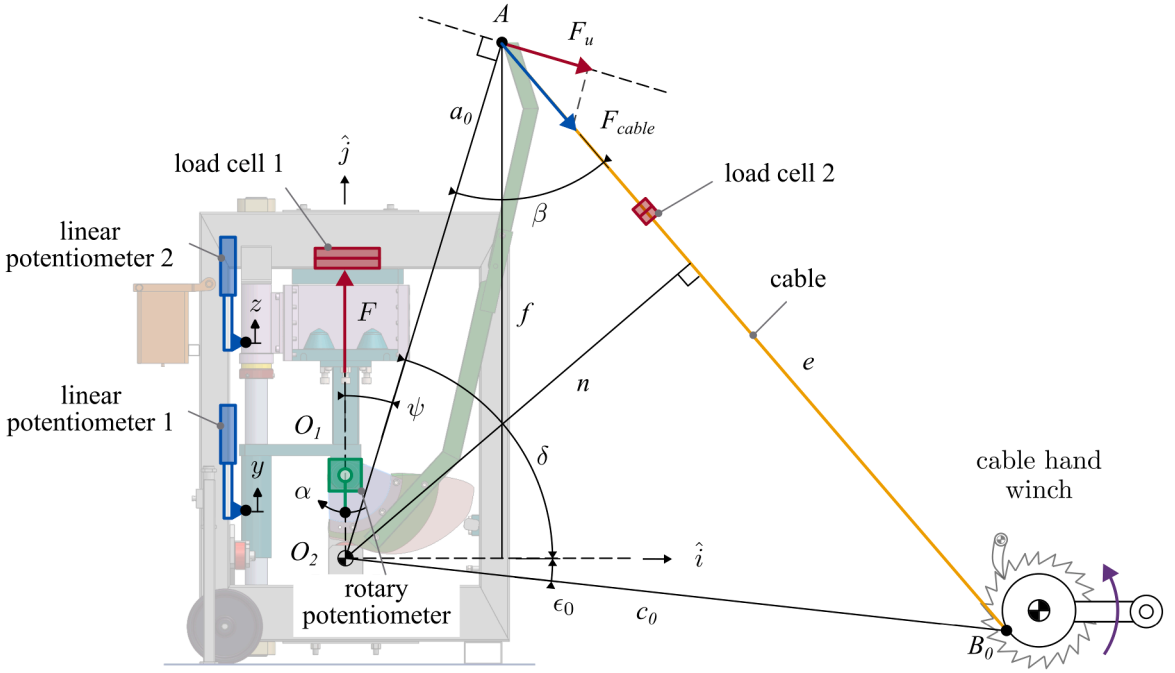


Fig. 15. Experimental setup scheme: the input lever is actuated through a cable that wraps around a passive pulley, the load cell 1 is used to measure F, the load cell 2 is used to measure F_{cable}, the linear potentiometer 1 measures the displacement y, the linear potentiometer 2 measures the displacement z, and the rotary potentiometer measure the rotation α. F_u is computed indirectly from F_{cable}.

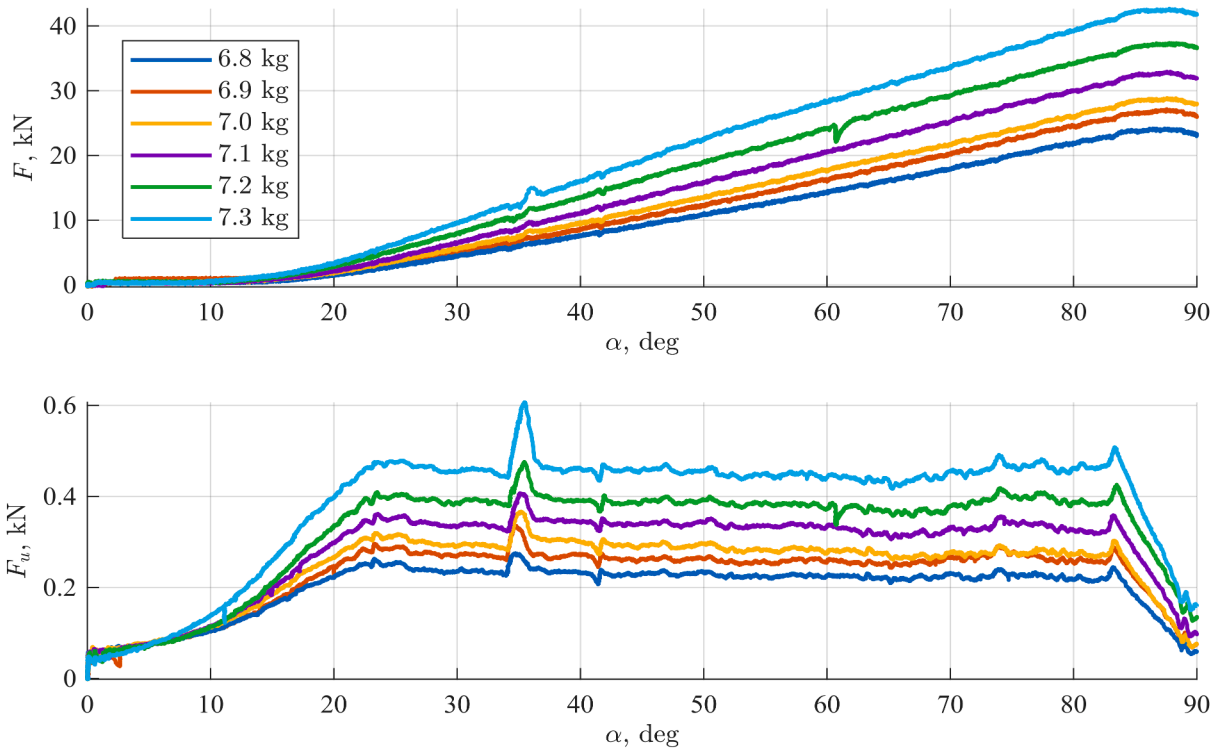


Fig. 16. Float-Ram experimental tests in laboratory: compression force F and user input force F_u as function of the input rotation α. The compression is repeated with different amounts of soil.

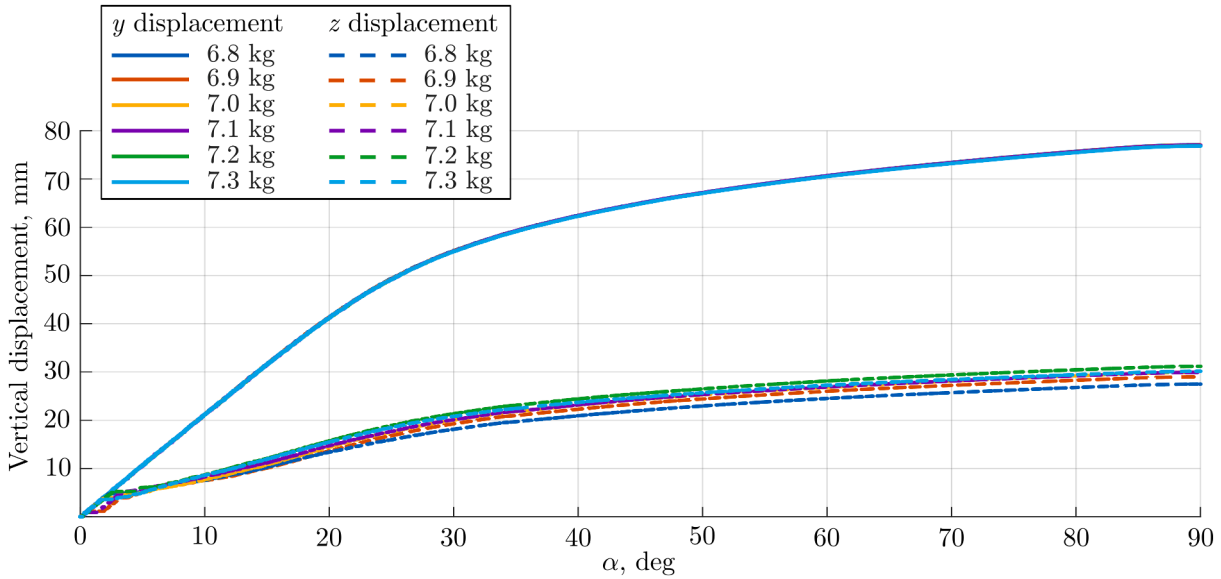


Fig. 17. Float-Ram experimental tests in laboratory: mold bottom plate vertical displacement y and floating mold vertical displacement z as function of the input rotation α. The compression is repeated with different amounts of soil.

F_u. As hypothesized during the design phase, the synthesized profile of the compression cam successfully compensates for the soil's exponential resistance, requiring a quasi-constant input force F_u from the operator to achieve the necessary compaction force.

Regarding the effectiveness of the bi-directional compression resulting from the adoption of the floating mold, interesting results are shown in Fig. 17, where the mold bottom plate vertical displacement y and the floating mold vertical displacement z are plotted as a function of the input rotation α. As expected, the vertical displacement y remains identical across all tests. This consistency is directly dictated by the cam profile, which mechanically imposes the vertical displacement of the mold bottom plate.

The compelling finding lies in the vertical displacement of the floating mold z. The average and standard deviation of the ratio between the maximum values of z and y is $38.4\% \pm 1.7\%$. As already mentioned in the first part of the paper, an ideal bi-directional compression would yield a floating mold displacement ratio of exactly 50%. Considering the friction between the soil mixture and the mold walls alongside the friction within the central cylindrical kinematic pair, this discrepancy is anticipated. However, a 38.4% ratio is a strong indicator that bi-directional compression is achieved. It is worth noticing, that Float-Ram achieves this result without relying on complex bi-directional mechanism as the one used in the Altech Geo50 brick press.

7. Social impact of the project

In addition to evaluating the quantitative aspects related to testing on the instrumented press, it is very interesting to assess the social impact of the technology and its application around the world. To develop and effectively implement a technological and social development project such as the Float-Ram press, it is necessary to bring together the work of multiple partners:

- a local community and a territory that clearly express a need and are able to adopt a new technology designed in accordance with the social, environmental, and economic conditions of the area;
- a group of researchers and technicians, often affiliated with a university, possessing both technical expertise and creativity;
- one or more organizations engaged in cooperation and development projects in vulnerable areas and capable of completing the project in collaboration with local communities.

In addition to these three elements, it is highly beneficial to have one or more individuals capable of connecting the different partners, including individuals who may belong to at least two of these groups.

The Float-Ram brick press has been used to construct buildings for residential purposes, kindergartens, and hospitals, and positive impacts on quality of life have been observed:

- The houses constructed in the Njombe region, while maintaining low construction costs through self-construction, are significantly healthier and more durable than traditional houses, such as those shown in Fig. 18 (a) and (b) shows the bricks irregular shape that can lead to structural problems of the building). In other words, it has been possible to achieve a positive impact on SDGs 10 and 11;
- The Mkiu kindergarten, shown in Fig. 18 (c), provided early childhood education in an area where no such opportunity previously existed. Over more than 10 years of activity, it has been observed that the young people who attended the kindergarten achieved better results in subsequent schools. The presence of a kindergarten also enabled parents to entrust their children to qualified



Fig. 18. (a) and (b) houses built with traditional and irregular fired mud brick, (c) Mkiu kindergarten, Tanzania, and (d) Ikelu nurse school, Tanzania made from Blocco Mattone CEB produced using Float-Ram.

educators while carrying out their work activities. Finally, children belonging to different religious backgrounds grew up together, laying the foundations for a multicultural and peaceful society. Furthermore, education at this kindergarten was also provided to girls, thereby contributing to a more equitable distribution of educational opportunities and the promotion of equal opportunities. In practice, a positive impact was observed on SDG 4 (Quality Education), SDG 5 (Gender Equality), SDG 10 (Reduced Inequalities), and SDG 16 (Peace).

- The construction of the nursing school in Ikelu (Fig. 18 (d)) was a fundamental step in bringing healthcare services to a remote area that had previously been completely underserved. The construction of a hospital alone would not have been sufficient to provide healthcare services in this area due to the reluctance of trained personnel from major cities to work in rural areas. For this reason, the idea of constructing a nursing school proved successful when combined with the construction of the adjacent hospital, as it enabled the training of healthcare personnel from the local area who would subsequently be willing to remain there because of their existing family and social ties. In summary, this project had a significant impact on SDG 3 (Good Health and Well-being).

8. Conclusion

This work presented the complete development, experimental validation, and field implementation of the Float-Ram manual press for producing interlocking stabilized compressed earth blocks (CEB) of the Blocco Mattone type. The adopted methodological approach successfully combined a rigorous analysis of the local needs of vulnerable communities with advanced, ergonomics-oriented mechanical engineering, resulting in an open and replicable technology transfer.

The primary findings and technical innovations resulting from this research can be summarized as follows. First, the introduction of the central cylindrical kinematic pair and the floating mold system enabled effective bidirectional compaction while eliminating mechanical complexity, dual-lever mechanisms, and high costs characteristic of previous-generation commercial presses (e.g., Altech Geo50). Then, the analytical design of the compression cam based on the exponential soil compaction law ($p = k_1 e^{k_2 c_r}$) successfully converted a moderate and nearly constant operator manual effort (≈ 300 N) into the high compaction force required. Optimizing the working trajectory reduces physical operator fatigue and ensures operational safety within a lever rotation range of only 90°. Moreover, laboratory tests conducted on a sensorized prototype across varying soil charge masses (6.8 kg – 7.3 kg) confirmed the validity of the mathematical models used for cam synthesis. The floating mold displacement ratio of $38.4\% \pm 1.7\%$ relative to the bottom plate translation confirms the attainment of genuine bidirectional compaction. The press integrates all manufacturing cycle stages (filling via an adjustable feeding drawer, pressing, and block ejection) into a single main assembly. The modular and foldable

structure ($800 \times 900 \times 1250$ mm in shipping configuration) is optimized for standard pallet transport and easy maneuverability via integrated wheels directly within informal construction sites.

Finally, the deployment of the Float-Ram press in Tanzania proved the capacity of appropriate technology to trigger self-sustaining processes of social empowerment. The construction of durable residential dwellings in Njombe, the integrated kindergarten in Mkiu, and the health training facility in Ikelu confirms a tangible impact on health improvement (SDG 3), educational access (SDG 4), gender equality (SDG 5), inequality reduction (SDG 10), and the creation of resilient, sustainable communities (SDG 11).

Although the cam synthesis in this paper is demonstrated using the specific compression curve of the "Blocco Mattone" soil mix, the underlying design methodology is fully generalizable to any manual compaction mechanism processing compressible materials (e.g., alternative soil-cement blends, agricultural residues, waste-stabilized composites, or powdered industrial media). The general design procedure follows a four-step framework:

1. Empirical resistance profiling: experimental static compression tests are conducted on the target material to establish its non-linear pressure-displacement characteristic $p(y_c)$ or force curve $F(y_c)$, where y_c is the material height reduction during compression.
2. Operator and ergonomic constraint definition: the desired operator effort profile (e.g., a constant target force F_{in} or torque T_{in}) and input motion types and stroke (e.g., rotational input motion with a maximum lever rotation angle α_{max}) are defined based on the ergonomic standards and application.
3. Analytical kinematic inversion: by applying the principle of virtual work, the instantaneous velocity ratio $y'(\alpha) = dy_c/d\alpha$ is derived, inverting the material's compaction profile into the required transmission ratio function. The resulting motion profile can be modified based on preference. For example, zero-resistance zones can be included to provide the operator with physical feedback about the completion of the compression phase.
4. Cam profile synthesis: Eqs. (12)–(14) are used to obtain the required cam profile.

This systematic workflow ensures that any non-linear material compaction law can be mapped into a prescribed, comfortable human-powered input without trial-and-error physical prototyping.

CRediT authorship contribution statement

Luigi Tagliavini: Writing – original draft, Visualization, Resources, Data curation; **Giuseppe Quaglia:** Writing – review & editing, Validation, Project administration, Investigation, Formal analysis, Conceptualization; **Walter Franco:** Writing – review & editing, Validation, Methodology, Investigation, Formal analysis; **Matteo Asteggiano:** Validation, Supervision, Investigation.

Declaration of competing interest

The authors declare that they have no known competing financial interests or personal relationships that could have appeared to influence the work reported in this paper.

Data availability

Data will be made available on request.

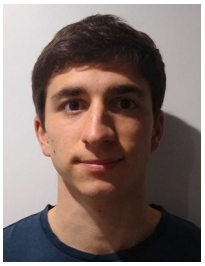
Supplementary material

Supplementary material associated with this article can be found in the online version at https://github.com/seromedises-PoliTo/Float-Ram-main.

References

[1] United Nations Human Settlements Programme, UN-Habitat: for a better urban future, 2026. https://unhabitat.org, Accessed: 27 May 2026.
[2] United Nations, Transforming our World: The 2030 Agenda for Sustainable Development, Resolution A/RES/70/1, United Nations General Assembly, 2015. Adopted on 25 September 2015.
[3] S. Economic, United Nations Department of and Affairs, The Sustainable Development Goals Report 2025, Report, United Nations, New York, USA, 2025.
[4] Habitat for Humanity International, Causes of Inadequate Housing in Latin America and the Caribbean, Regional Study, Habitat for Humanity, Latin America and the Caribbean Regional Office, 2007. Global Housing Research Initiative.
[5] M. Foti (Ed.), Tecnologie per tutti-Soluzioni semplici e a basso costo per l'habitat, Scuola di specializzazione in" Tecnologia, architettura e città nei Paesi in via di sviluppo" del Politecnico di Torino, Servizio Diocesano Terzo Mondo, Torino, (2003).
[6] S. Kean, From the bottom up, Sci. 327 (5966) (2010) 638–639. https://doi.org/10.1126/science.327.5966.638.
[7] W. Franco, F. Iarussi, G. Quaglia, Human powered press for producing straw bales for use in construction during post-emergency conditions, Biosyst. Eng. 150 (2016) 170–181.
[8] W. Franco, G. Quaglia, C. Ferraresi, Experimentally based design of a manually operated baler for straw bale construction, in: Advances in Italian Mechanism Science: Proceedings of the First International Conference of IFToMM Italy, Springer, 2016, pp. 307–314.
[9] A. Piemonte, Haiti| 1| Foyer d'accueil aux enfants démunis d'Haiti, in: III Congress of the University Network for Development Cooperation (CUCS Torino 2013), Torino, 2013, pp. 19–21.
[10] G. Scudo, B. Narici, C.M.L. Talamo, et al., Costruire con La Terra: Tecniche Costruttive, Campi di Utilizzo e Prestazioni, Esselibri, 2001.
[11] Mattone su Mattone, Associazione Mattone su Mattone – Progetto di solidarietà e accoglienza, 2026, Accessed: 27 May 2026.
[12] H. Guillaud, H. Guillaud, T. Joffroy, P. Odul, Compressed Earth Blocks: Manual of Design and Construction, vol. 2, Vieweg Eschborn, 1995.
[13] B.V.V. Reddy, Design of a manual press for the production of compacted stabilized soil blocks, Curr. Sci. 1 (2015) 1651–1659.

[14] K. Mukerji, Soil Block Presses, Technical Report, German Appropriate Technology Exchange (GATE), 1988.
[15] V. Rigassi, Compressed Earth Blocks: Manual of Production, CRATerre-EAG / GATE-GTZ, 1995.
[16] S. Deboucha, R. Hashim, A review on bricks and stabilized compressed earth blocks, Sci. Res. Essays 6 (3) (2011) 499–506.
[17] O.A. Ibitoye, A critical analysis of interlocking stabilized soil blocks (ISSB) in residential architecture: a case study, Int. J. Multidiscip. Res. Growth Eval. 6 (3) (2025) 562–569.
[18] S. Talibi, J. Page, C. Djelal, M. Waqif, L. Saâdi, Study of earth-based materials for manufacturing compaction process, J. Build. Eng. 64 (2023) 105546.
[19] A.A. Thennarasan Latha, B. Murugesan, B. Skariah Thomas, Compressed earth block reinforced with sisal fiber and stabilized with cement: manual compaction procedure and influence of addition on mechanical properties, Mater. Today: Proc. (2023). https://doi.org/10.1016/j.matpr.2023.04.373.
[20] B.B. Zewudie, Experimental study on the production and mechanical behavior of compressed lime-cement-stabilized interlock soil blocks, Adv. Mater. Sci. Eng. 2023 (2023) 2933398. https://doi.org/10.1155/2023/2933398.
[21] C. Ferraresi, W. Franco, G. Quaglia, Concept and design of Float-Ram: A new human powered press for compressed earth blocks, in: ASME International Mechanical Engineering Congress and Exposition, volume 58462, American Society of Mechanical Engineers, 2017, p. V011T15A025.
[22] G. Quaglia, C. Ferraresi, W. Franco, Float-Ram: A sustainable machine for buildings made by compressed earth blocks, in: G. Quaglia, A. Gasparetto, V. Petuya, G. Carbone (Eds.), Proceedings of I4SDG Workshop 2021, Springer International Publishing, Cham, 2022, pp. 99–109. https://doi.org/10.1007/978-3-030-87383-7_11.
[23] M. Olivier, Le Matériau Terre, Compactage, Comportement, Application aux Structures en bloc sur terre, thesis, Lyon, INSA, 1994.
[24] P.L. Magnani, G. Ruggeri, et al., Meccanismi per Macchine Automatiche, Utet, 1986.



Luigi Tagliavini is an Assistant Professor (RTDA) in the Department of Mechanical and Aerospace Engineering (DIMEAS) at Politecnico di Torino, Italy. He received his B.Sc. in Mechanical Engineering in 2018 at Università degli Studi di Ferrara, his M.Sc. in Mechanical Engineering in 2020 at Politecnico di Torino, and his Ph.D. in Mechanical Engineering in 2024 at Politecnico di Torino. His research interest lies in the design and the development of innovative mobile service robots and assistive technologies.



Giuseppe Quaglia is a full professor of Applied Mechanics at Politecnico di Torino, Italy. His scientific activity is mainly related to: energy saving, renewable energy and sustainability, vehicle dynamic and systems, robotics and mechatronics, automation, actuators and mechanisms, device for disabled people and biomedical applications, appropriate technologies and systems for sustainable human development. Moreover, he had the scientific responsibility of competitive National and International research projects, awarded through a peer-review process. Prof. Quaglia was leading research projects between the Politecnico di Torino and industries like Texa automotive testing s.r.l., C.F. Gomma, SKF Industrie s.p.a., m.t.m. srl, Carmec s.r.l., Freudenberg Sealing Technologies sas, Corcos, EDISON S.p.A., Alba robot. The results of applied research and technological transfer are evidenced by the presence of 16 patents, indicating the originality and innovative nature of the research activity. He is: Chair of Technical Committee for Sustainable Energy Systems of IFToMM, Member of SIRI council, (Italian Association of Robotics and Automation), Member of Management Board of “Politecnico Interdipartmental Center for Service Robotics” (PIC4SeR), Chair of IFToMM Cross Disciplinary Group 1: Securing our Future Environment - Air, Water, Energy, Coordinator of Inclusion and Equal Opportunities Politecnico di Torino Green Team, Director of Politecnico di Torino Japan Hub.



Walter Franco is full professor in Applied Mechanics at the Department of Mechanical and Aerospace Engineering (DIMEAS) of the Politecnico di Torino, where he teaches Humanitarian Engineering, Technologies for Sustainable Development, and Mechanics for Design. His research focuses on appropriate technologies-specifically the development of intermediate machines and devices for marginalized communities or those undergoing socio-ecological transitions-as well as the functional analysis of machines and mechanisms of historical interest.



Matteo Asteggiano was born in Bra (CN) in 1954. He earned a degree in mechanical engineering from Politecnico di Torino and was licensed to practice in 1979. He has been married to Sandra since 1978 and is the father of three children and grandfather of nine grandchildren. Together with his wife, between 1979 and 1982, he spent several years doing civilian volunteer work in Madagascar, where he later helped found the Zanantsika Association-along with other volunteers-which continues to operate in schools, helping thousands of the poorest children. He taught science in high schools, worked at various courts as an expert reconstructing the dynamics of serious traffic accidents, served as director and administrator of MTM srl-now a world leader in the automotive gas sector-and was a partner in MTM Hydro and Sinergie Srl. At the same time, he developed business ventures focused on products with an extremely low environmental impact and built an eco-friendly hotel. Over the past 20 years or so, he has collaborated extensively with Politecnico di Torino on the development of equipment for scientific research and has provided consulting services and technical materials to various companies. Hobbies: cycling tours and Argentine tango.